On the energy cost of robustness and resiliency in IP networks

B. Addis [b], A. Capone [a,*], G. Carello [a], L.G. Gianoli [a,c], B. Sansò [c]

[a] *Politecnico di Milano, Dipartimento di Elettronica, Informazione e Bioingegneria, Italy*
[b] *LORIA (UMR 7503 CNRS), Université de Lorraine, INRIA Nancy-Grand Est, France*
[c] *École Polytechnique de Montréal, Département de Génie Électrique, Canada*

Received 17 December 2013
Received in revised form 12 September 2014
Accepted 1 October 2014
Available online 17 October 2014

1. Introduction

Network operators and device manufacturers agree that the energy consumption of communication networks can no longer be neglected [1]. According to recent estimates [2], the worldwide electricity consumption of telecom operators has grown from 150 TW h/y in 2007 to 260 TW h/y in 2012, which accounts for almost 3% of the total worldwide consumption.

This growing consumption has stimulated the development of new strategies to increase the energy efficiency of communications networks, with particular focus on IP networks [3–5]. In this context, remarkable improvements can be obtained with energy-aware strategies for network management and traffic engineering that dynamically optimize the network configuration by putting to sleep some network components (line cards and nodes) while

* Corresponding author.
E-mail addresses: bernardetta.addis@loria.fr (B. Addis), capone@elet.polimi.it (A. Capone), giuliana.carello@polimi.it (G. Carello), gianoli@elet.polimi.it (L.G. Gianoli), brunilde.sanso@polymtl.ca (B. Sansò).

using the remaining active elements to route the traffic [4,6–10].

The aim of energy-aware management is to adjust both the network topology and the available capacity to varying traffic levels in order to keep active only the resources that are essential for the actual load. It is basically a dynamic redesign of the network that takes as input the predicted or measured traffic pattern. Management approaches differ depending on the strategy to select the sleeping/active parts, on the way to optimize the routing through the active network, on the reconfiguration timescales considered, i.e. off-line [6,11] or on-line [13,14] and on how closely traffic variations can be followed by network reconfigurations.

It is quite evident that the best energy performance can be obtained by bespoke tailoring the network capacity to the traffic level. On the other hand, there are several important features that depend on the spare capacity available in the network when working conditions are different from the expected. Protection techniques are widely used to guarantee the network resiliency to failures of links (or device interface serving a link) and nodes. In case of failure, the affected traffic is rerouted on the surviving part of the network. To guarantee the possibility of accommodating the affected traffic on alternative paths, it is necessary to make some spare capacity available so as to cope with these anomalous situations. Furthermore, traffic can be different from what is expected due to uncertainty associated with traffic estimations or quick deviations that cannot be followed by monitoring and measurement techniques. Then, networks should be designed to be robust to these variations. Thus, spare capacity is necessary to compensate for traffic fluctuations around the nominal value.

There is clearly a trade off between energy consumption and level of resilience and/or robustness of the network. However, the way protection techniques and robustness strategies are integrated within the energy-aware network management methodologies is fundamental to determine their energy cost. Further, if technologies to fast reactivate sleeping elements are available, energy-efficient approaches can be developed which integrate recovering from failures within the network energy management framework.

The fundamental question that we tackle in this paper is whether it is possible to design a network with embedded reliability, survivability and robustness and still reduce energy consumption. We also want to evaluate the energy cost of protection and robustness considering different available techniques. Therefore, we introduce a novel framework for survivable and robust energy-aware network management that builds on our recent work on multi-period energy-aware network management in IP networks [11].[1] The central idea is to introduce dedicated and shared protection into energy-aware IP network management models and add the notion of network robustness [18] to traffic variations as well.

[1] Preliminary results have been presented in [15–17].

The proposed energy-aware framework takes into account topology and traffic information to determine the network configuration, i.e. demand routing and device states (on/sleep) in a planning horizon. The framework is based on Mixed-Integer Linear Programming (MILP) models, which differ with respect to the chosen resilience features. As Internet traffic is characterized by a slow dynamic and a periodic daily behavior, we assume a time-horizon of a single day periodicity. The day is divided into time-periods in which the average level of traffic is expected to be almost constant. For each time period, a different network configuration can be chosen. The routing is adjusted so that both router chassis and line cards that are not necessary for the support of the incoming level of traffic are put to sleep. Quality of Service (QoS) is guaranteed by means of explicit constraints on the maximum link utilization. Inter-period constraints are imposed to limit the number of switching on/off of each line card, as they reduce the device lifetime. The power needed to reactivate sleeping chassis is taken into account.

Two key elements of the framework refer to how network survivability and energy consumption are treated. Network survivability is guaranteed by protection schemes. A backup path is assigned to each traffic demand and spare capacity is reserved to the backup path itself. Regarding spare capacity allocation, dedicated and share protection are considered. For energy consumption of backup paths, two alternatives are considered: a so called *classic* protection, where all network devices carrying at least one path are kept active, and the *smart* protection according to which line cards that carry only backup traffic are deactivated in normal operation, and therefore do not consume energy. When these features are combined, four variants of the problem are obtained: classic dedicated, smart dedicated, classic shared and smart shared.

Robust variants of the models are also proposed to account for the uncertainty of traffic demands. Each traffic demand is uncertain, and is assumed to vary in a symmetric interval. Under this assumption, the cardinality-constrained approach for Robust Optimization proposed in [18] is applied. The additional amount of spare capacity reserved to cope with traffic variations (i.e. the robustness degree of the solution) can be adjusted by tuning a few input parameters. To effectively manage the implementation of both primary and backup paths, we consider IP networks operating with Multi Protocol Label Switching (MPLS), according to which one or more dedicated paths are explicitly defined for each traffic demand. Along with the exact MILP formulation, we also present some heuristic methods to efficiently solve network instances with up to 50 nodes and 176 links.

The reminder of the paper is organized as follows. In Section 2 the state-of-the-art literature on energy-aware network management is reviewed and the novelties of our work are underlined. In Section 3 the most relevant aspects of the proposed energy-aware framework are discussed, while in Sections 4–6 the MILP formulations taking into account both survivability and robustness issues are presented. The resolution methods and computational results are extensively discussed in Sections 7 and 8, respectively. Finally, some concluding remarks are reported in Section 9.

2. Related work

From the first seminal work by Gupta and Singh [19], a great attention has been devoted to make Internet greener (see [9,10] for a survey).

Besides improving the energy efficiency of networking devices, a promising strategy to reduce Internet power consumption is represented by energy-aware network management, whose aim is to adapt the network consumption to the incoming level of traffic by efficiently optimizing the network configuration [3].

If the fixed energy consumption component of the network devices is comparable to the load proportional one (currently it typically accounts for 90% of the total consumption [7]), substantial energy savings can be achieved by putting to sleep the redundant network devices [20].

It is shown [21] that the slow dynamic and the periodicity of Internet traffic can be naturally exploited to significantly reduce the network energy consumption by means of a few optimal network configurations. Based on such observation, in this study we address a multi-period energy-aware network management problem to plan in advance the configuration for the coming days. We con-sider inter-period constraints, thus the problem cannot be split into several single period independent subprob-lems. Inter-period constraints are needed to capture important features such as the impact of reactivation on device lifetime.

In addition to multi-periodicity, this work deeply differs from state-of-the-art literature because it formalizes and discusses a comprehensive planning framework which jointly considers a number of features that have been typically managed in an independent way: (i) sleeping-capable devices, (ii) MPLS per-flow (flow-based) single path routing, (iii) network links composed by multiple line cards (bundled links), (iv) resilience to single-link failures and (v) robustness to traffic variations.

Despite the growing number of publications on energy-aware network management during the last years, to the best of our knowledge, multi-period planning with inter-period constraints has been not previously considered but in two papers [11,22], where an exact MILP formula-tion is proposed and heuristic to jointly determine the daily switching pattern for the network devices and the routing configuration which minimize the overall network consumption.

A two-period planning problem is addressed in [23], where, however, no inter period constraints are considered. The authors propose to implement a fully active network configuration during normal/peak traffic periods and to adopt a reduced green topology along low traffic hours (e.g. night hours). A two-stage heuristic is proposed: a greedy to identify the green network configuration, and a local-search to determine its applicability window.

Points (i) and (ii) have been addressed by several work aiming at quickly determining the energy-aware configuration of a network topology according to the observed traffic matrix (see e.g. [13,24–26]). Both [24,25] propose a similar greedy algorithm which, starting from a fully active network, check the possibility of putting to sleep each network link and node one by one. A different perspective is considered in [13], where some local-search online procedures to perform the so-called *Energy-Aware Traffic Engineering* are presented: the framework aims at dynamically optimizing the current network consumption by adjusting the amount of traffic sent by each edge router through a pre-determined set of paths. A distributed online approach is presented in [26], where a framework called DAISIES is used to dynamically update the Label Switched Paths (LSP) defined by MPLS whenever their utilization cross some pre-defined utilization thresholds. The new LSPs are defined as the shortest paths determined by link weights related to both energy consumption and link utilization. All these approaches are meant to be run in an on-line fashion (e.g. every 5 or 10 min). The above approaches do not consider any issue related to network stability or protection mechanisms.

Points (i), (ii) and (iii) have been addressed by the online optimization frameworks presented in [27–29]. Given a network topology and a traffic matrix, Fisher et al. [27] propose three different greedy-based heuristics which determine if a line card can be put to sleep by solving an LP formulation to maximize the network spare capacity. A similar idea is developed in [28], where a given line card can be put to sleep if the link utilization is below a given threshold. Paths are computed via k-shortest-path algorithms. Finally, in [29] a heuristic based on genetic algorithm and particle swarm optimization is presented to evaluate how the capacity and the number of each bundle (called energy levels in the paper) may impact the size of the energy savings. In these works only link (line cards) can be put to sleep.

For the sake of completeness we refer the reader to [6,30–33] for other work on sleep-based energy aware network management which consider alternative routing schemes.

Point (iv), i.e. network resilience to failures, was first introduced in the context of green networking in [34]. The majority of the work on resilient and energy-aware network management focuses on the optical (physical layer) instead of the IP layer [35–39]. Working at the optical layer changes the target of the optimization, which is repre-sented by the optical light-paths, and requires the introduc-tion of additional components such as optical amplifiers, optical cross-connects and optical transponders.

In [35,36], primary light-paths are protected through a dedicated scheme according to which a backup light-path is established for each primary light-path. Primary and backup paths have the same bandwidth requirement. An ILP formulation based on a precomputed set of paths is presented and tested in [35] for relatively small instances. Three greedy heuristics are presented in [36]. They address a restated version of the problem defined in [35] where network link which carry only backup resources can be put to sleep. The light-path of each connection is computed by considering a path cost related to both energy and blocking aspects.

Network resilience to single link failures is guaranteed through shared protection in [37,38]. Except for the protection scheme, the problems discussed in [37,38] are very similar to that presented in [36]: in both papers the

authors propose a different iterative algorithm to perform admission control of the incoming connections which, from time to time, perform the Yen's [38] or the Dijkstra [37] shortest path algorithm to find an admissible pair of primary-backup light-paths.

A different perspective is assumed in [39], where the proposed management strategy for network resilience does not rely on backup paths, but on the definition of a budget on the minimum reliability required by each connection. The reliability of each path is computed by considering a measure of the failure probability observed on each link. The authors propose a heuristic to minimize the power consumption by optimizing the network routing and blocking the connection that cannot be served with the required reliability.

In [40–42] the optimization is performed at the IP level. In [40] the authors present different MILP formulations to reduce network consumption while guaranteeing link protection or demand protection. Experimentations have been conducted on 8-node networks. A multi-rate scenario with six different rate/energy states for each device is discussed in [41], where three MILP formulations considering dedicated (two formulations, the second one with the possibility to put to sleep network elements carrying only backup paths) and shared (one formulation) protection. Finally, the Lagrangian based algorithm proposed in [42] implements link protection through NotVia IP fast re-route so as to maximize the energy savings and guarantee network resilience to single node failures.

None of the previous work considers two different maximum link utilization thresholds to account for the congestion allowed during normal operation periods and in fault scenarios.

We refer the reader to [43] for a general survey on multi-period network optimization and survivable network design.

To the best of our knowledge, point (v), i.e. robustness, has been considered only in a preliminary work [17] and in [44]. In [44] the amount of transmitted traffic is reduced exploiting redundancy elimination (packets carrying the same contents are transmitted in a reduced form), thus increasing the number of elements that can be put to sleep. In addition to network routing and device states, the problem aims at deciding where to install the high power consuming hardware required to perform the redundancy elimination. In [44] the uncertainty affects the redundancy degree of each demand, while we consider uncertainty affecting the demands amount. We refer the reader to [18,45] for general surveys on robust optimization applied in both general and network contexts.

3. Energy management, robustness and survivability

We here present the key elements of our proposed approach and discuss their interactions and roles when managing the system to reduce energy consumption and, at the same time, to guarantee a certain level of protection against failures and traffic variations. This preliminary high level description of the framework is intended to give an overview of the issues that motived our mathematical models that are then presented in detail in next section. For this reason, at the end of this section, we included a visual example on a small network that can help under-stand more easily the impact of resiliency and robustness on energy efficiency.

3.1. Energy management

Given a backbone IP network composed of routers (chassis) and links (line cards), we consider the problem of planning in advance (i.e. off-line) both routing and topology configurations so as to minimize the daily network con-sumption, while guaranteeing the normal network operation, in terms of both QoS and resiliency to failures. Power consumption is reduced by efficiently exploiting a subset of network equipment to route traffic demands and by putting to sleep the remaining idle devices.

To efficiently adapt the network configuration to the traffic level, we split the considered time horizon, a single day for instance, in multiple time periods, or scenarios, characterized by a given traffic level (see Fig. 1). The time period division is performed by analyzing the daily traffic profiles (see for instance [46]) typically observed or estimated by the network provider. The traffic demand in each time period is, for the sake of simplicity, represented by a single average estimated traffic matrix called *traffic scenario*. The demand profile associated to the considered time horizon is cyclically repeated.

3.2. Demand robustness

Due to the regular daily/weekly behavior of the traffic profiles [46], network providers exploit direct [47] and indirect methods [48], to estimate traffic matrices in normal conditions. Since real traffic matrices naturally deviate around predicted values, we use robust optimization techniques to reserve enough spare bandwidth to satisfy unpredictable peaks of traffic. The basic idea is to adapt the modeling proposed in [18] to our energy aware-problem. According to [18], each traffic demand can vary into a close symmetric interval centered on its average traffic value. A set of tunable parameters is used to adjust the

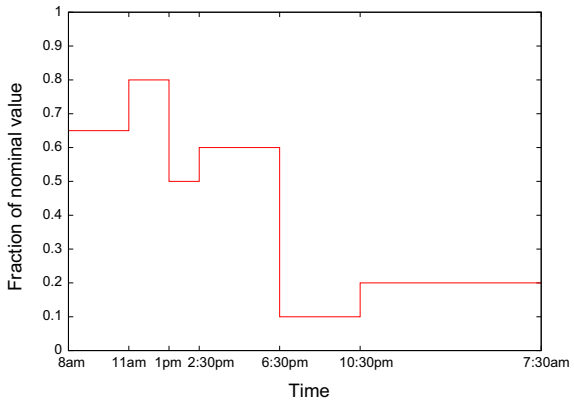

Fig. 1. Traffic scenarios.

robustness degree of the solutions by varying the total deviation allowed on each link.

In our multi-period modeling framework the consumption over the entire time horizon is minimized by jointly considering all traffic scenarios. Inter-period constraints are introduced to take into account the energy cost of powering on a particular device and to preserve network stability. For instance, we impose a so-called card-reliability constraint to preserve the line-card lifetime by limiting the number of switching on of a single line card over the considered time horizon.

3.3. Survivability

Network resiliency to failures is provided by considering two different kinds of protection schemes, i.e. dedicated and shared, which allow to protect the network in case of break down of a single link. Since multiple link failures and single node failures are very unlikely events, they have not been considered in this paper. Both dedicated and shared protection require the definition of a primary path and a backup path for each traffic demand. The latter is used to transmit data only after a link break down in the primary path. The two schemes have different advantages and disadvantages. Dedicated protection reserves demand capacity on both primary and backup paths. This results in an excessive amount of reserved backup resources that, in case of single link-failure, will never be completely exploited. In shared protection, the backup paths corresponding to two link-disjoint primary paths share the same backup capacity when routed on the same link, in fact they will never be activated simultaneously. In this case the amount of backup capacity required is the maximum of the two traffic amounts. Due to the smaller amount of backup resources required, shared protection naturally allows to reduce the energy consumption.

3.4. A visual example

In this subsection we illustrate with an example different outcomes of our modeling framework depending on the considered protection and robustness features. They are presented in Fig. 2(a)–(d). In the figures, link capacity is assumed to be two units and there are four traffic demands each requesting one unit of traffic.

Fig. 2(a) represents the simple case for which no protection schemes are implemented. We can see that there are 4 nodes and 10 bidirectional links to put to sleep, making this case the most energy-efficient.

When the uncertainty of traffic demands is explicitly considered (Fig. 2(b)) the system cannot share any link between the four traffic demands routed in the network. Thus, three more nodes and six more links have to be activated, increasing the consumption with respect to the Simple case given above.

In case of dedicated protection (Fig. 2(c)), additional links and nodes have to be switched on (three more nodes and six more links) to carry the backup paths. Note that, since each backup path has the same bandwidth requirement of the primary one, the two demands $G-I$ cannot be routed on the links already used by the backup paths of the two demands $D-F$. However, by implementing shared protection (Fig. 2(d)), it is possible to sensibly reduce the consumption due to protection and put to sleep two more nodes and two more links w.r.t. the dedicated case. These savings can be achieved because shared protection allows to share the backup resources on the links used by the backup paths (links $G-H$ and $H-I$), since the primary paths of demands $D-F$ are link disjoint from the primary paths of demands $G-I$.

To further reduce the network power consumption, in addition to the *classic* approach just described, we also investigate a slightly modified variant, that we call *smart* version, in which line cards carrying only backup paths can be switched off. In fact, since line cards can be rapidly reactivated (in the order of milliseconds) from the sleeping state [49], it is reasonable to assume that those used only by backup paths are powered only when required by the occurrence of a failure, thus having negligible consumption. It is worth pointing out that the same scheme cannot be applied to network routers because a chassis switch on requires a significant time. Further, QoS is guaranteed by imposing a limitation on the maximum allowed link utilization. Since the occurrence of a link failure is very unlikely, we opted to include a second higher utilization threshold enable only when backup resources are exploited. Allowing the network to operate with a higher but still reasonable congestion during the very limited failure intervals we are able to further increase the energy savings.

As shown in Fig. 2(e) and (f), the smart protection allows to further reduce the network consumption by switching off an additional number of links. With respect to the corresponding classic cases, with the dedicated-smart protection six more links can be put to sleep, whereas with shared-smart protection the additional sleeping links are four. With the smart strategies, it can be advantageous to use different links to carry primary and backup paths, as this allows to switch off link devices that are used only for backup.

By combining the different features, such as robustness or survivability, eight different versions of the problem can be defined, i.e. *simple*, *robust*, *dedicated-classic*, *shared-classic*, *dedicated-smart*, *shared-smart*, *robust plus dedicated-classic* and *robust plus dedicated-smart*. In the following sections, we describe the considered versions and their mathematical formulations (the constraints describing each problem are summarized in Table 3).

4. Reference model for energy management

Let us consider a backbone IP network. Each router is composed of a chassis of capacity ψ and a set of line cards each of capacity γ. Duplex links connect routers. To guarantee the connectivity of link (i,j), n_{ij} line cards dedicated to link (i,j) must be available on both routers i and j. Therefore, each link has multiple operating states based on the number of powered-on line cards. Since links have the same bandwidth in both directions, the number of powered-on line cards must be the same in both directions. We can represent the network with a symmetric directed graph $G(N,A)$, where N represents the sets of chassis, and A represents the bidirectional links and their associated line cards.

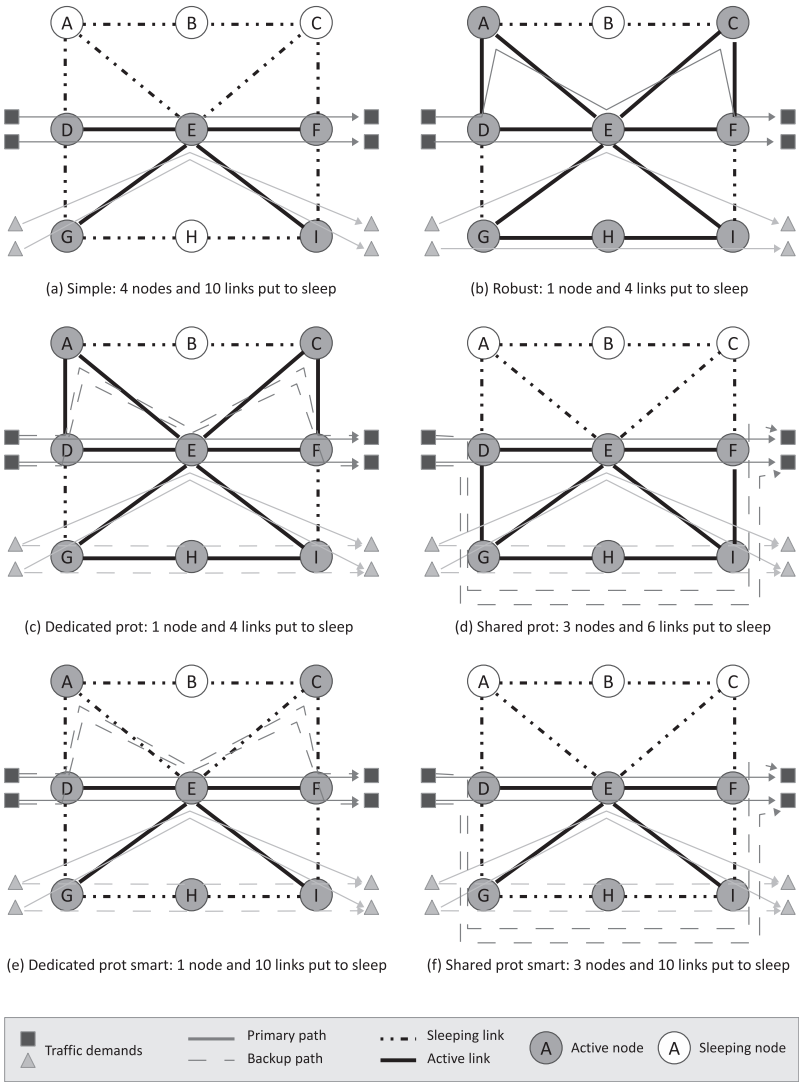

Fig. 2. Energy consumption minimization vs resilience requirements.

The maximum utilization level allowed on each link to guarantee the required QoS is denoted by the positive real parameter $\mu_a \in [0,1]$. Therefore the available bandwidth on one card is given by $\mu_a \gamma$. When all the line cards connected to a given router are in the stand-by mode, the router chassis can be put to sleep too.

Due to the multi-period nature of the addressed problem, the considered daily time horizon is split in a set S of time periods: each time period $\sigma \in S$ has duration h_σ. The network traffic is represented by a set of traffic demands D, where each demand $d \in D$ is described by a source node o_d, a destination node t_d, and the amount of demand q_d^σ that has to be satisfied during period σ.

Concerning energy consumption, let π_{ij} and $\bar{\pi}$ be positive real parameters representing the hourly power consumption, respectively, of a single card installed on link (i,j), and of a chassis. The reactivation of a chassis typically causes a consumption spike: let parameter δ denote the additional power consumption (normalized with respect to hourly one) associated with a chassis switching-on. As for the card reactivation, we assume that the associated energy consumption is negligible. Nevertheless, to preserve the lifetime and the reliability of network equipment, a single line card cannot be switched on more than ε times along an entire day.

The parameters are summarized in Table 1.

The multi-period energy-aware network management problem asks to determine the routing for each demand, and which cards and chassis are switched-on in each time period, with the aim of reducing the overall energy consumption.

We first introduce the reference MILP formulation for the multi-period energy-aware network management previously presented in [11], then, in the following sections, we describe the modeling of the resiliency and robustness features.

The problems can be modeled using several sets of variables. Demand d routing in scenario σ is described through

Table 1
Parameters.

Param.	Description
ψ	Chassis maximum capacity
$\bar{\pi}$	Chassis power consumption
δ	Chassis switch on energy consumption
n_{ij}	Number of available cards on link (i,j)
γ	Per card capacity
π_{ij}	Card power consumption
ε	Max number of allowed card switch-on
μ_a	Max link utilization for primary traffic
μ_b	Max link utilization during failures
o_d	Origin of demand d
t_d	Destination of demand d
q_d^σ	Demand value on scenario σ
h_σ	Duration of scenario σ

binary variables $x_{ij}^{d\sigma}$, which are equal to 1 if the routing path of demand d is routed on link (i,j) in scenario σ. The status of the chassis in each scenario is described by a binary variable y_i^σ, which is equal to 1 if the chassis i is on during scenario σ, and 0 otherwise. The power consumption for the reactivation of chassis j at the beginning of scenario σ is represented by continuous non negative variable z_j^σ. The number of active line cards on link (i,j) during period σ is represented by an integer variable $w_{ij}^\sigma \in [0, n_{ij}]$. The number of activations of a card is described by auxiliary binary variable u_{ijk}^σ, which is equal to one if the k-th card linking nodes i and j is powered on in scenario σ.

The variables are summarized in Table 2.

The problem (*simple*) is represented as follows:

$$\min \sum_{\sigma\in S}\left[h_\sigma \sum_{j\in N}\bar{\pi}y_j^\sigma + \sum_{(i,j)\in A}\pi_{ij}w_{ij}^\sigma\right) + \sum_{j\in N}z_j^\sigma\Bigg]$$

$$\sum_{(i,j)\in A}x_{ij}^{d\sigma} - \sum_{(j,i)\in A}x_{ji}^{d\sigma} = b_i^d, \qquad \forall\ \sigma\in S,\quad i\in N,\quad d\in D \quad (1)$$

$$\sum_{(i,j)\in A}\sum_{d\in D}q_d^\sigma x_{ij}^{d\sigma} +$$

$$\sum_{(j,i)\in A}\sum_{d\in D}q_d^\sigma x_{ji}^{d\sigma} \leqslant \psi y_j^\sigma, \qquad \forall\ \sigma\in S,\quad j\in N \quad (2)$$

$$\sum_{d\in D}q_d^\sigma x_{ij}^{d\sigma} \leqslant \mu_a\gamma w_{ij}^\sigma, \qquad \forall\ \sigma\in S,\quad (i,j)\in A \quad (3)$$

$$w_{ij}^\sigma = w_{ji}^\sigma, \qquad \forall\ \sigma\in S,\quad (i,j)\in A \quad (4)$$

$$z_j^\sigma \geqslant \delta\bar{\pi}\left(y_j^\sigma - y_j^{\sigma-1}\right), \qquad \forall\ \sigma\in S, j\in N \quad (5)$$

$$\sum_{\sigma\in S}u_{ijk}^\sigma \leqslant \varepsilon, \qquad \forall\quad (i,j)\in A,\quad k\in[1,n_{ij}] \quad (6)$$

$$\sum_{k=1}^{n_{ij}}u_{ijk}^\sigma \geqslant w_{ij}^\sigma - w_{ij}^{\sigma-1}, \qquad \forall\quad \sigma\in S,\quad (i,j)\in A \quad (7)$$

The objective function aims at minimizing the daily energy consumption. It is the sum of three terms taking into account, respectively, the energy consumed by the router chassis in each scenario $\sum_{j\in N}\bar{\pi}y_j^\sigma$, the energy used by the line cards $\sum_{(i,j)\in A}\pi_{ij}w_{ij}^\sigma$, and the energy consumed when chassis are reactivated $\sum_{j\in N}z_j^\sigma$.

4.1. Routing constraints

The routing constraints (1) represent flow conservation constraints. As routing variables $x_{ji}^{d\sigma}$ are binary, they describe the single path unsplittable routing typically used in MPLS networks. The right hand side parameter b_i^d is 1 if $i = o_d$, -1 if $i = t_d$ and 0 in all the other cases.

Table 2
Variables.

Var.	Description
x_{ij}^d	Primary path routing
ζ_{ij}^d	Backup path routing
y_j^σ	Chassis status
w_{ij}^σ	Link/Card status
u_{ijk}^σ	Card change of state
z_j^σ	Chassis switch on energy consumption
$g_{ijkl}^{d\sigma}$	Joint primary and backup path routing

4.2. Chassis status constraints

Constraints (2) force the proper value of chassis status variables: if a demand is routed through chassis i the left hand side of Eq. (2) is strictly positive and therefore y_i^σ must be equal to one. On the other hand, if y_i^σ is equal to zero, no demand can be routed through chassis i. The constraints guarantee also that the chassis capacity ψ is not exceeded.

4.3. Card and link status and capacity

As for the chassis, the status of cards is set through a set of constraints, which also guarantee that the bandwidth available on each link, which depends on the number of active cards w_{ij}^σ, is not exceeded (3). To guarantee a suitable level of QoS, the total used capacity is at most a fraction μ_a of the available one. Besides, constraints (4) force to keep activated the same number of line cards in both the direction of each link, so as to guarantee network stability.

4.4. Chassis and card activation constraints

Constraints (5) set the value of variables z_j^σ. The number of card activations is limited by constraints (6), while the proper value of variables u_{ijk}^σ is set by constraints (7).

4.5. Note on complexity

We assess the problem complexity by reduction from the Directed Two-commodity Integral Flow (DTIF) which is known to be NP-complete in its decision form (problem ND38 in [12]).

DTIF, in decision form, is defined as follows: given a directed graph $\underline{G} = (\underline{N}, \underline{A})$, two pairs of nodes $s_1,\ t_1$ and $s_2,\ t_2$, with $s_1,\ t_1,\ s_2,\ t_2 \in N$, an integer non-negative capacity for each arc $c(i,j)$, and two integer non-negative requirements R_1 and R_2, are there two flow functions $f_1, f_2 : \underline{A} \to Z_0^+$ such that:

- for each arc $(i,j) \in \underline{A}\ f_1(i,j) + f_2(i,j) \leqslant c(i,j)$,
- for each $v \neq s_i,\ t_i,\ i = 1,2$ flow is conserved at v,
- for $i = 1,2$ the net flow into t_i under flow f_i is at least R_i?

Table 3
Problem constraints summary.

Problem	Constraints
simple	(1), (2), (4)–(7), (3)
robust	(1), (2), (4)–(7), (25)–(28)
dedicated-classic	*simple*, (8)–(12)
dedicated-smart	*simple*, (8)–(11), (15)
shared-classic	*simple*, (8)–(11), (13), (14)
shared-smart	*simple*, (8)–(11), (13), (16)
robust plus dedicated-classic	*robust*, (8)–(11), robust version of (12)
robust plus dedicated-smart	*robust*, (8)–(11), robust version of (15)

For the NP-completeness proof we refer to the decision version of the multi-period energy-aware network management problem in the simple version (*simple* in the following).

The decision version is defined as follows: given the parameters and constraints as described in Section 4, are there a path for each demand and a power state pattern for cards and chassis such that the overall energy consumption is below a threshold κ?

To asses NP-completeness of *simple* we first prove that it is in *NP*. Given a set of paths and a power state pattern for chassis and cards, representing an assignment of values to variables of the problem formulation, it is possible to verify in polynomial time if the paths are feasible and compatible with the power state pattern and if the overall consumption is below the given threshold κ (the formulations has a polynomial number of constraints).

Then we reduce DTIF to *simple*, by building in polynomial time an instance (I_{simple}) of *simple* given any instance of DTIF (I_{DTIF}). The graph of I_{simple} is built as follows: $N = \underline{N}$ and $A = \underline{A} \cup \{a_1\} \cup \{a_2\}$, where a_1 and a_2 are the direct arcs connecting s_1 to t_1 and s_2 to t_2, respectively. We consider only one time interval, namely $|S| = 1$, and $h_1 = 1$. Therefore, all the parameters associated to the multi-period feature are now not relevant (δ, ϵ). We consider two demands, namely $|D| = 2$, and $o_i = s_i$, $t_i = t_i$ and $q_i^1 = R_i$ for $i = 1, 2$. For each $(i, j) \in A$ $\underline{n}_{ij} = c_{ij}$ and $\pi_{ij} = 0$. As for a_1 and a_2, for $i = 1, 2$, $n_{a_i} = R_i$ and $\pi_{a_i} = M$, where $M > 0$. Card capacity γ is equal to 1 for all the arcs, while $\mu_a = 1$. For each node $i \in N$ $\psi_i = R_1 + R_2$; $\bar{\pi} = 0$. If there exists a solution of I_{simple} whose overall energy consumption is equal to 0, then it is possible to route the two demands in I_{DTIF} on the original graph. In fact, the routing found solving *simple* uses only arcs that belong to $\underline{A}$. Otherwise, if there exists no solution of I_{simple} whose energy consumption is below M, then there exist no two flows f_1 and f_2 satisfying the requirements of DTIF, in fact at least one of the two demands is routed on the auxiliary arcs a_1, a_2.

5. Modeling resilience

In the considered protection schemes, two disjoint paths, a primary and a backup, must be determined for each demand. Modeling a protection scheme requires the addition of both routing variables and flow conservation constraints. The backup paths are represented by binary variables $\xi_{ij}^{d\sigma}$, which are equal to one if backup path of demand d is routed on link (i,j) in scenario σ. Some constraints describing resiliency are common for all the considered schemes, while the card capacity constraints are different for each scheme. The common constraints are modeled as follows:

$$\sum_{(i,j)\in A} \xi_{ij}^{d\sigma} - \sum_{(j,i)\in A} \xi_{ji}^{d\sigma} = b_i^d, \qquad \forall \sigma \in S, \quad i \in N, \quad d \in D \tag{8}$$

$$x_{ij}^{d\sigma} + \xi_{ij}^{d\sigma} \leqslant 1, \qquad \forall \sigma \in S, \quad (i,j) \in A, \quad d \in D \tag{9}$$

$$x_{ij}^{d\sigma} + \xi_{ji}^{d\sigma} \leqslant 1, \qquad \forall \sigma \in S, \quad (i,j) \in A, \quad d \in D \tag{10}$$

$$\sum_{(i,j)\in A}\sum_{d\in D} q_d^\sigma \left(x_{ij}^{d\sigma} + \xi_{ij}^{d\sigma}\right) + \sum_{(j,i)\in A}\sum_{d\in D} q_d^\sigma \left(x_{ji}^{d\sigma} + \xi_{ji}^{d\sigma}\right) \leqslant \psi y_j^\sigma, \quad \forall \sigma \in S, \quad j \in N \tag{11}$$

5.1. Backup path routing constraints

As the variables describing the primary path $x_{ij}^{d\sigma}$, the backup path variables must satisfy the flow conservation constraints (8). In addition, the primary and backup path of a given demand d must be link disjoint, as guaranteed by constraints (9) and (10).

5.2. Chassis status constraints

Chassis capacity constraints (11) take into account the resources reserved for primary and backup paths. Besides, they guarantee the suitable behavior of chassis activation variables.

5.3. Card capacity constraints

Concerning the line card capacity, two values of the maximum card capacity fraction are considered to provide the network QoS both in case of normal network operation and of single link failure. If no failure occurs, the value of maximum card capacity fraction is μ_a, and the constraints are inequalities (3). For the single link failure, the value of maximum card capacity fraction is μ_b, which represents the maximum utilization allowed in case of failure when both primary and backup paths are used. The value μ_b is greater or equal than μ_a, and it is used by the network operator to find the desired trade off between resilience and consumption. It allows the network congestion to be slightly deteriorated during the very short and unlikely periods in which a single link failure occurs, in order to achieve higher savings in normal conditions.

The capacity needed on each link is different according to the different adopted protection schemes (12) and (14).

5.3.1. Dedicated protection case

According to the dedicated protection scheme, the capacity constraint (12) states that the sum of the demands whose primary and backup paths are routed on a link cannot exceed the link available capacity.

$$\sum_{d\in D} q_d^\sigma \left(x_{ij}^{d\sigma} + \xi_{ij}^{d\sigma}\right) \leqslant \mu_b \gamma w_{ij}^\sigma, \qquad \forall \sigma \in S, \quad (i,j) \in A \tag{12}$$

5.3.2. Shared protection case

According to the shared protection scheme, the capacity on a link must be greater or equal than the sum of the demands whose primary path is routed on the considered link plus the worst backup capacity due to different failures. Such case is computed by evaluating the impact of each failure and selecting the highest one. The impact of a failure is given by the sum of the demands whose backup paths are routed on the considered link and whose primary paths fall if the considered failure occurs. To correctly model the backup capacity to be reserved on each link, a set of binary variables $g^{d\sigma}_{ijkl}$ is introduced. A binary variable $g^{d\sigma}_{ijkl}$ is defined for each pair of links (i,j) and (k,l), each demand d and each scenario σ, and it is equal to 1 if the demand must be rerouted on link (i,j) if link (k,l) fails, i.e. the traffic demand d is served by a primary and a backup paths routed, respectively, on link (i,j) and link (k,l) in scenario σ. The shared protection case requires the following constraints:

$$g^{d\sigma}_{ijkl} \geqslant x^{d\sigma}_{ij} + \xi^{d\sigma}_{kl} - 1, \quad \forall \sigma \in S, \ (i,j),(k,l) \in A, \ d \in D \tag{13}$$

$$\sum_{d \in D} q^{\sigma}_{d} \left(x^{d\sigma}_{ij} + g^{d\sigma}_{klij} \right) \leqslant \mu_b \gamma w^{\sigma}_{ij}, \quad \forall \sigma \in S, \ (i,j),(k,l) \in A \tag{14}$$

Constraints (13) force the correct value of $g^{d\sigma}_{ijkl}$. The impact of failure (k,l) on link (i,j) is computed by constraints (14), which allow to protect the network (i.e. to reserve enough capacity) by reserving on each link enough backup bandwidth to cope with the worst-case single link failure.

5.4. The smart consumption variant

The smart protection variant exploit the possibility of reactivating sleeping line cards in a few milliseconds and therefore the possibility of putting to sleep line cards that carry only backup paths during normal network operation. Such new feature of dynamic network can be modeled by replacing constraints (12) with constraints (15) for the dedicated protection case.

$$\sum_{d \in D} q^{\sigma}_{d} \left(x^{d\sigma}_{ij} + \xi^{d\sigma}_{ij} \right) \leqslant \mu_b \gamma n_{ij} y^{\sigma}_{j}, \qquad \forall \sigma \in S, \quad (i,j) \in A \tag{15}$$

Similarly, constraints (14) must be replaced with (16) for the shared protection case.

$$\sum_{d \in D} q^{\sigma}_{d} \left(x^{d\sigma}_{ij} + g^{d\sigma}_{klij} \right) \leqslant \mu_b \gamma n_{ij} y^{\sigma}_{j}, \qquad \forall \sigma \in S, \quad (i,j),(k,l) \in A \tag{16}$$

Constraints (15) and (16) guarantee that the total available capacity on each link (γn_{ij}) is not exceeded by the sum of primary and backup traffic routed on it, when all the cards are switched on. However, the status of cards is forced by primary paths only, as described by (3). Note that the sleeping cards carrying backup paths have to be connected to an active chassis.

6. Modeling robustness to traffic variations

Uncertainty arise in the problem when the demand is described by an uncertain parameter q^{σ}_{d}. To deal with such uncertainty, we apply the cardinality-constrained approach proposed in [18]. The approach exploits the idea that all the uncertain parameters are very unlikely to assume simultaneously their worst possible value. The uncertain parameters are supposed to vary in the interval $[\bar{q}^{\sigma}_{d} - \hat{q}^{\sigma}_{d}, \bar{q}^{\sigma}_{d} + \hat{q}^{\sigma}_{d}]$, where $\bar{q}^{\sigma}_{d}$ and $\hat{q}^{\sigma}_{d}$ represent, respectively, the expected traffic value and the maximal variation considered during period σ. In [18] uncertainty is dealt as follows. Any solution is feasible if, for each card capacity constraint associated to link (i,j) and scenario σ, at most Γ^{σ}_{ij}[2] demands, among those routed on (i,j), assume their maximum value $\bar{q}^{\sigma}_{d} + \hat{q}^{\sigma}_{d}$, while all the others assume their expected one, $\bar{q}^{\sigma}_{d}$. Parameters $\Gamma^{\sigma}_{ij} \in [0, |D|]$ can be used to tune the required robustness degree by limiting the number of traffic demands that are considered uncertain. In this way, we do not limit ourselves to perform a trivial worst-case optimization. Instead, by using Γ^{σ}_{ij} values smaller than $|D|$, we can ignore the most unlikely realizations where all the traffic demands routed on a link (i,j) assume simultaneously the maximal deviation, achieving in this way higher level of energy savings.

Uncertain parameters have an impact on constraints (3).[3] For each such constraint a set U^{σ}_{ij} is defined as the set of demands which assume their maximum possible amount. The cardinality of U^{σ}_{ij} is at most Γ^{σ}_{ij}. The robust counterpart of constraints (3) is:

$$\sum_{d \in D} \bar{q}^{\sigma}_{d} x^{d\sigma}_{ij} + \max_{\{U^{\sigma}_{ij} \subseteq D, \, |U^{\sigma}_{ij}| \leqslant \lfloor \Gamma^{\sigma}_{ij} \rfloor\}} \left\{ \sum_{d \in U^{\sigma}_{ij}} \hat{q}^{\sigma}_{d} x^{d\sigma}_{ij} \right\} \leqslant \mu \gamma w^{\sigma}_{ij}, \qquad \forall \sigma \in S, \quad (i,j) \in A \tag{17}$$

Let Θ^{σ}_{ij} represent the worst case additional traffic to be considered on link (i,j) during period σ, *i.e.* $\Theta^{\sigma}_{ij} = \max_{\{U^{\sigma}_{ij} \subseteq D, \ |U^{\sigma}_{ij}| \leqslant \lfloor \Gamma^{\sigma}_{ij} \rfloor\}} \left\{ \sum_{d \in U^{\sigma}_{ij}} \hat{q}^{\sigma}_{d} x^{d\sigma}_{ij} \right\}$. The value of Θ^{σ}_{ij} can be computed through dualization.

Given a solution represented by the routing variables $\bar{x}^{d\sigma}_{ij}$, the value of Θ^{σ}_{ij} can be computed solving the following linear programming problem:

$$\Theta^{\sigma}_{ij} = \max \sum_{d \in D} \hat{q}^{\sigma}_{d} \bar{x}^{d\sigma}_{ij} u^{d\sigma}_{ij} \tag{18}$$

s.t.

$$\sum_{d \in D} u^{d\sigma}_{ij} \leqslant \Gamma^{\sigma}_{ij} \tag{19}$$

$$0 \leqslant u^{d\sigma}_{ij} \leqslant 1, \quad \forall d \in D \tag{20}$$

Let us denote by ϵ^{σ}_{ij} and $l^{d\sigma}_{ij}$ the dual variables associated to constraints (19) and (20) respectively. The dual of prob-lem (18)–(20) is the following:

$$\min \sum_{d \in D} l^{d\sigma}_{ij} + \Gamma^{\sigma}_{ij} \epsilon^{\sigma}_{ij} \tag{21}$$

s.t.

$$\epsilon^{\sigma}_{ij} + l^{d\sigma}_{ij} \geqslant \hat{q}^{\sigma}_{d} \bar{x}^{d\sigma}_{ij}, \quad \forall d \in D \tag{22}$$

$$l^{d\sigma}_{ij} \geqslant 0, \quad \forall d \in D \tag{23}$$

$$\epsilon^{\sigma}_{ij} \geqslant 0 \tag{24}$$

[2] For the sake of conciseness, we assume parameters Γ_{ij} to be integer. However a more general case, in which they can also continuous, can be easily dealt with, as described in [18].

[3] Although uncertain parameters are present in constraint (2), uncertainty has not an impact on such constraints, as such constraints force the status of chassis variables rather than limiting the overall used capacity.

According to the duality properties, the optimal primal and dual objective functions coincide and thus the robust constraints (17) can be replaced with the following constraints:

$$\sum_{d\in D}\bar{q}_d^{\sigma}x_{ij}^{d\sigma}+\sum_{d\in D}l_{ij}^{d\sigma}+\Gamma_{ij}^{\sigma}\epsilon_{ij}^{\sigma}\leqslant\mu\gamma w_{ij}^{\sigma}, \quad \forall\sigma\in S,\quad (i,j)\in A \tag{25}$$

$$\epsilon_{ij}^{\sigma}+l_{ij}^{d\sigma}\geqslant\hat{q}_d^{\sigma}x_{ij}^{d\sigma},\qquad \forall\sigma\in S,\quad (i,j)\in A,\quad d\in D \tag{26}$$

$$l_{ij}^{d\sigma}\geqslant 0,\qquad \forall\sigma\in S,\quad (i,j)\in A,\quad d\in D \tag{27}$$

$$\epsilon_{ij}^{\sigma}\geqslant 0,\qquad \forall\sigma\in S,\quad (i,j)\in A \tag{28}$$

It is very important to point out that the robust approach can be naturally applied as well to the protected case.

7. Resolution methods

All the MILP formulations previously presented can be treated by state-of-the-art solvers. In our case we experimented with CPLEX 12.5.0.0 using the AMPL modeling language and setting a resolution time limit of 1 h. Due to the time-limit and the complexity of the models, the final solution may be sub-optimal.

Since, for scalability reasons, the MILP formulations can be efficiently solved for instances with less than 20 nodes, 50 links and 50 demands, to solve larger instances (up to 50 nodes and 300 demands) we developed different MILP based heuristics exploiting variants of the original MILP formulations.

Algorithm 1. Single Time Period Heuristic.

```
Input: G Topology, D Traffic Matrix,
       S Time Periods, T Problem Type
Output: BestSolution
if UseRestrictedPaths then
    ComputePrecomputedPaths(G, Ω)
end
BestConsumption = bigM
foreach σ_start ∈ S do
    CurrentPeriod = σ_start
    NextPeriod = Next(σ_start)
    while NextPeriod ≠ σ_start do
        Solve SinglePeriodMILP(T,CurrentPeriod)
        Store CardState parameters
        Update CurrentConsumption
        CurrentPeriod = NextPeriod
        NextPeriod = Next(CurrentPeriod)
    end
    if CurrentConsumption ≤ BestConsumption then
        BestSolution = CurrentSolution
    end
end
```

7.1. Single time period heuristic

The Single Time Period Heuristic (STPH) presented in [11] can be adapted to solve both the protected and the robust cases. The basic idea is to deal with each time period separately and sequentially, by solving a reduced MILP model derived from the main one, where only variables and constraints concerning the considered interval are taken into account. It is worth pointing out that some group of constraints are used to correctly evaluate the energy consumed to reactivate a chassis, and keep track of the number of switching on each line card along all the previous periods. Card reliability constraints are satisfied by keeping activated all the line cards already switched on ε times in the previously optimized time intervals. Since the choice of the starting period may influence the final solution, the algorithm is repeated $|S|$ times, starting at each iterations from a different scenario. The pseudo-code of STPH is reported in Algorithm 1.

7.2. Path restriction

To further speed up the single time period heuristic, we developed a new version of the algorithm, i.e. single time period heuristic with restricted paths (STPH-RP) based on the use of a pre-computed restricted set of paths assigned to each traffic demand.

To formalize the restricted-path variants of the complete MILP formulations, let P^d represent the set of pre-computed paths assigned to demand d, and let χ_p^d and λ_p^d be the binary variables equal to 1 when path $p\in P^d$ is exploited by demand d, as primary path and backup path, respectively. In the single time period heuristic we consider one single scenario at the time, thus scenario index σ is not necessary.

The following set of constraints replace the flow conservation constraints (1) to force each demand to use a single primary path:

$$\sum_{p\in P^d}\chi_p^d=1,\quad \forall d\in D \tag{29}$$

Similarly, for the protected case, flow conservation constraints of backup path (8) are replaced by:

$$\sum_{p\in P^d}\lambda_p^d=1,\quad \forall d\in D \tag{30}$$

Then, considering that:

$$x_{ij}^d=\sum_{p\in P^d:(i,j)\subset p}\lambda_p^d,\qquad \forall(i,j)\in A,\quad d\in D \tag{31}$$

$$\xi_{ij}^d=\sum_{p\in P^d:(i,j)\subset p}\chi_p^d,\qquad \forall(i,j)\in A,\quad d\in D \tag{32}$$

all the original constraints have to be modified by replacing the x_{ij}^d and ξ_{ij}^d variables with the corresponding path-based expression.

The pre-computed paths of each demand are generated by means of the following procedure. First, for each demand $d\in D$, an LP formulation is solved to compute the maximum flow m_d that can be routed from node o_d to node t_d when each link has unitary capacity. Then, being Ω an integer positive parameter, the precomputed paths are obtained by performing Ω iterations of the following multi-stage algorithm: (i) a random weight is assigned to each link, (ii) for each demand d, m_d shortest paths (disjoint if possible) are computed by solving a minimum cost

flow LP formulation, (iii) a minimum cost spanning tree is computed with the Kruskal algorithm, (iv) a single path for each demand is extracted from the links belonging to the spanning tree. At the end of the procedure $\Omega m_d + \Omega$ paths are available. It is worth pointing out that the two different strategies used to generate the paths allow to find both disjoint paths to better achieve load balancing and implement the protection schemes, and very correlated paths (with a lot of common links) to minimize the consumption.

7.3. Warm starting

Due to the extreme complexity of the shared protection model, we developed a procedure to warm start CPLEX (when solving both the multi-period exact model and each single period of the heuristic) with a solution rapidly obtained by solving the dedicated protection formulation with a limited time-limit. In case of the exact formulation the time limit is typically set to 3 min (with 57 min left to the resolution of the main model). For the heuristic the solution obtained for the previous scenario is given as input to solver, by properly initializing the variables of the considered time periods with the values of those of the previous one. Both warm-starts are implemented in CPLEX using the option `send_statuses 2`. In the heuristic, due to some AMPL code constraints, the resolution of each single period is equally split between the dedicated protection warm start and the shared protection model. Note that each feasible solution of the dedicated protection is naturally feasible for the shared protection.

8. Computational results

Several computational tests were performed to evaluate both the impact of the different proposed strategies and the performance of the resolution methods. All the experiments were carried out on machines equipped with Intel i7 processors with 4 core and multi-thread 8x, and 8 Gb of RAM. In what follows, test-bed and instance characteristics are described in Section 8.1, the behavior of each strategy is exhaustively discussed in Section 8.2 and, finally, extensive results on the largest instances are analyzed in Section 8.3.

8.1. The test-bed

We tested both exact and heuristic methods using four network topologies provided by the SND Library (SNDLib) [50], i.e. `polska`, `nobel-germany`, `nobel-eu` and `germany`.

The summary of the instances features is reported in Tables 5 and 6. In Table 5, columns $|N| - |N_c|$, $|A|$ and $|D|$ represent the number of nodes and core nodes, the number of unidirectional links and the number of traffic demands, respectively. In Table 6, columns *ID*, *Net*, *equip* and *sce-nario* represent the instance label, the network topology, the equipment configuration and the traffic scenario, respectively.

In each test instance all routers are assumed to be equipped with the same type of chassis and the same type of cards. However, we experimented with three different configuration cases, *alfa*, *delta*, and *eta*, wherein the chassis technology is always the same, while the type of cards is varied (but the same technology is used for all the cards in a given instance). Chassis and card details are reported in Table 4. The network nodes are equally and randomly divided between core routers and edge routers. Notice that only core routers can be put to sleep, since they are neither source nor destination of any traffic demand.

Table 4
Overview of different network configurations.

Case	Device	Capacity	Hourly cons. (W)
–	Chassis Juniper M10i	16 Gbps	86.4
alfa	FE 4 ports	400 Mbps	6.8
delta	OC-3c 1 port	155 Mbps	18.6
eta	GE 1 port	1 Gbps	7.3

Table 5
Test instances – networks.

Net	$\|N\| - \|N_c\|$	$\|A\|$	$\|D\|$
polska	12–6	36	15
nobel-ger	17–9	42	21
nobel-eu	28–14	82	90
germany	50–25	176	182

Traffic matrices have been derived by those provided by the SNDLib. The nominal values ρ_d have been computed by scaling the SNDLib matrices with a fixed parameter $\varpi^{\mu_b}_{\mu_a}$. The chosen value of $\varpi^{\mu_b}_{\mu_a}$ is the highest value such that the matrix obtained multiplying the SNDLib values by $\varpi^{\mu_b}_{\mu_a}$ can be routed in the real full active network with protection (dedicated or shared), while respecting the maximum utilization in normal conditions μ_a, and the maximum utilization in failure conditions μ_b. In the majority of our tests we used matrices scaled for $\varpi^{85\%}_{50\%}$ computed by considering dedicated protection. That is, we used μ_a (link max-utilization due to primary paths) equal to 50% and μ_b (link max-utilization due to both primary and backup paths) equal to 85%.

We split a single day in six traffic periods corresponding to the following time intervals: (1) 8 a.m.–11 a.m., (2) 11 a.m.–1 p.m., (3) 1 p.m.–2.30 p.m., (4) 2.30 p.m.–6.30 p.m., (5) 6.30 p.m.–10.30 p.m., (6) 10.30 p.m.–8 a.m. We experimented with four different traffic scenarios (column *scenario*). The first three, i.e `a`, `b`, and `c`, were generated by considering traffic values q^σ_d distributed uniformly as a fraction r^σ_d of nominal value ρ_d. In particular we considered $q^\sigma_d = r^\sigma_d \rho_d$, where parameter r^σ_d is generated according to the uniform distribution $\mathcal{N}(\bar{r}^\sigma_d + \hat{r}^\sigma_d, \bar{r}^\sigma_d - \hat{r}^\sigma_d)$. The average values $\bar{r}^\sigma_d$ were chosen according to the traffic profile of Fig. 1, the variation $\hat{r}^\sigma_d$ is chosen as 0.2.[4]

In the fourth traffic scenario, namely `aver` (see Table 6), all the r^σ_d are equal to the average values $\bar{r}^\sigma_d$. This last scenario was used to compare with the robust approaches.

[4] Negative values are rounded up to value zero.

Table 6
Test instances – devices and scenarios.

ID	Net-conf	*equip*	*scenario*	ID	Net	*equip*	*scenario*
1	polska	alfa	a	25	nobel-eu	alfa	a
2	polska	alfa	b	26	nobel-eu	alfa	b
3	polska	alfa	c	27	nobel-eu	alfa	c
4	polska	alfa	aver	28	nobel-eu	alfa	aver
5	polska	delta	a	29	nobel-eu	delta	a
6	polska	delta	b	30	nobel-eu	delta	b
7	polska	delta	c	31	nobel-eu	delta	c
8	polska	delta	aver	32	nobel-eu	delta	aver
9	polska	eta	a	33	nobel-eu	eta	a
10	polska	eta	b	34	nobel-eu	eta	b
11	polska	eta	c	35	nobel-eu	eta	c
12	polska	eta	aver	36	nobel-eu	eta	aver
13	nobel-ger	alfa	a	37	germany	alfa	a
14	nobel-ger	alfa	b	38	germany	alfa	b
15	nobel-ger	alfa	c	39	germany	alfa	c
16	nobel-ger	alfa	aver	40	germany	alfa	aver
17	nobel-ger	delta	a	41	germany	delta	a
18	nobel-ger	delta	b	42	germany	delta	b
19	nobel-ger	delta	c	43	germany	delta	c
20	nobel-ger	delta	aver	44	germany	delta	aver
21	nobel-ger	eta	a	45	germany	eta	a
22	nobel-ger	eta	b	46	germany	eta	b
23	nobel-ger	eta	c	47	germany	eta	c
24	nobel-ger	eta	aver	48	germany	eta	aver

To evaluate the performance of the robust approaches, we experimented with uncertainty sets of different sizes, i.e. by setting $\hat{r}_d^\sigma$ = 0.05, 0.10, 0.15, 0.20, and by tuning the robustness degree of the solutions, i.e. by varying each Γ_{ij}^σ from 0 (no robustness) to 5 (high level of robustness in the considered instances).

As for the remaining parameters, we set δ (chassis switching-on normalized consumption) equal to 0.25, ε (switching-on limit) equal to 1, and n_{ij} (number of cards in link (i,j)) equal to 2 for each link.

8.2. Savings vs protection/robustness

First we aim at pointing out the impact of the different features provided according to the protection/robustness strategy considered, i.e. *simple*, *robust*, *dedicated-classic*, *shared-classic dedicated-smart*, *shared-smart*, *robust plus dedicated-classic* and *robust plus dedicated-smart*. The expected trade-off between energy savings and network survivability/robustness is reported in Fig. 3. Starting from the simple energy-aware problem with no protec-tion and no robustness, we expect the energy consumption of the network to gradually increase if we increase the protection/robustness (P/R) level. At the first P/R level we put the *robust* approach with no protection, which, by varying the robustness parameters $\Gamma_{ij}^{d\sigma}$ and the size of the uncertainty intervals $\hat{r}_d^\sigma$, allows to allocate additional resources to cope with traffic variations. Then, we find, in sequence, the *shared-smart* strategy and the *dedicated-smart* one. Although shared protection guarantees the same degree of survivability of the dedicated one, with single link failures, we consider it less conservative because it produces solutions with, in general, less spare capacity available. Clearly, the larger the spare capacity, the higher the capability of the network to react to failures and other unexpected events. Moving towards the right side of the graph, we first meet the *shared-classic* and the *dedicated-classic* strategies, and finally the two *robust plus dedicated* protection. Classic schemes are considered more conservative than smart ones because all backup capacity is kept activated. It is worth to notice that, in term of consumption, switching off the backup links with dedicated protection is more efficient than the complex shared protection scheme (see detailed results in following subsections). *Robust plus shared* strategies are not reported due to the high computational effort required, that does not allow to solve even the smallest instances in a reasonable time.

To confirm the expected behavior we considered twelve instances associated to the smallest network, `polska`, and solved the MILP formulation of each problem with a time limit of one hour. The effectiveness of the computing methods, i.e. computing times, solution optimality, absolute savings, are evaluated, as well.

8.2.1. Robust strategy

Let us first analyze the results reported in Table 7 for the *robust* case. Columns $\hat{r}$ and *TL* represent the size of the demand deviation and the resolution time-limit, respectively. Then, for each instance, column $\%E_c$ represents the ratio between the energy consumption of the optimized network with respect to the energy consumed by the fully active network. The robustness degree of the solution is evaluated on a set of randomly generated scenarios. We generated 10,000 random traffic scenarios where the $r^{d\sigma}$ parameters were generated with the uniform distribution $\mathcal{N}(\bar{r}_d^\sigma + \hat{r}_d^\sigma, \bar{r}_d^\sigma - \hat{r}_d^\sigma)$. For each generated scenario we then tested the optimized solutions by routing the random demands and verifying the violation of the capacity robust constraints. Columns $\%_{infeas}$ and Max_{dev} represent the percentage of random scenarios wherein at least one capacity constraint was violated, and the largest positive difference between the observed and the allowed maximum utilization, respectively. A solution can be considered completely robust if $\%_{infeas}$ = 0%. Results clearly show that, thanks to the robust model, the optimized solutions can be completely immunized to traffic variations by using the robust parameter Γ equal to 4 (four demands considered uncertain on each link). Most importantly, the absolute energy consumption increase necessary to reserve additional resources is smaller, in average, than 1%, and, in the worst case (instance 4 with $\bar{r}$ = 0.2) equal to 2.8%. It is worth pointing out that (i) the nominal solution ($\Gamma = 0$) is largely unreliable, with $\%_{infeas}$ 95.6% and Max_{dev} = 35.6% in the worst case (instance 12 with $\bar{r}_d^\sigma$ = 0.2), (ii) the increase of Γ produces a gradual improvement of the robustness degree, as expected, (iii) the increase of the uncertainty interval force the model to reserve more resources and reduce the potential savings. The results analysis suggests that robustness has a relatively small energetic cost and allows to greatly reduce the violations of the maximum utilization constraint due to traffic variations, which is a very crucial aspect for any off-line network management approach.

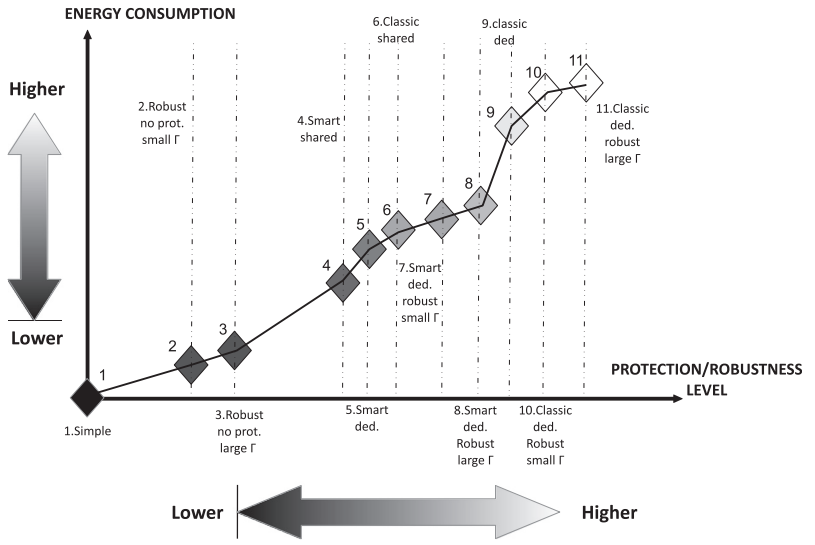

Fig. 3. Savings vs protection/robustness.

Table 7
Robustness analysis for the solutions obtained by the robust exact model with no protection with 1 h time limit on `polska` instances.

ID	$\dot{r}$	*TL* (h)	Polska – exact model – robust approach with no protection														
			$\Gamma = 0$			$\Gamma = 1$			$\Gamma = 2$			$\Gamma = 3$			$\Gamma = 4$		
			$\%E_c$	$\%_{infeas}$	$Max_{dev}(\%)$	$\%E_c$	$\%_{infeas}$	Max_{dev} (%)	$\%E_c$	$\%_{infeas}$	Max_{dev} (%)	$\%E_c$	$\%_{infeas}$	Max_{dev} (%)	$\%E_c$	$\%_{infeas}$	Max_{dev} (%)
4	0.05	1	60.6	42.33	6.57	60.7	9.91	0.78	60.9	0.00	0.00	60.9	0.00	0.00	60.9	0.00	0.00
4	0.10	1	60.6	81.69	16.32	60.9	10.18	2.56	60.9	0.09	1.73	60.9	0.09	1.73	60.9	0.00	0.00
4	0.15	1	60.6	92.32	24.64	60.9	15.27	9.22	61.4	0.27	4.76	61.4	0.27	4.76	61.4	0.00	0.00
4	0.20	1	60.6	95.60	32.30	60.9	32.89	19.19	62.4	0.04	1.26	62.4	0.04	1.26	63.4	0.00	0.00
8	0.05	1	50.6	40.80	6.24	50.8	10.48	0.78	51.0	0.00	0.00	51.0	0.00	0.00	51.0	0.00	0.00
8	0.10	1	50.6	78.39	14.83	51.0	1.29	0.61	51.0	0.00	0.00	51.0	0.00	0.00	51.0	0.00	0.00
8	0.15	1	50.6	88.64	24.24	51.0	9.49	8.85	51.5	0.46	4.89	51.5	0.46	4.89	51.6	0.00	0.00
8	0.20	1	50.6	93.95	33.59	51.0	27.62	19.41	52.6	0.05	1.10	52.6	0.05	1.10	53.2	0.00	0.00
12	0.05	1	60.0	41.37	7.05	60.1	4.71	0.70	60.3	0.00	0.00	60.3	0.00	0.00	60.3	0.00	0.00
12	0.10	1	60.0	78.73	15.41	60.3	11.23	2.34	60.3	0.00	0.00	60.3	0.00	0.00	60.5	0.00	0.00
12	0.15	1	60.0	88.49	24.41	60.3	6.87	9.17	60.7	0.41	4.92	60.7	0.41	4.92	60.8	0.00	0.00
12	0.20	1	60.0	94.12	35.61	60.3	40.13	18.45	61.6	0.01	0.20	61.6	0.01	0.20	62.5	0.00	0.00

8.2.2. Protection strategies: energy efficiency

Results concerning the protection scheme models are reported in Tables 8–10. In Table 8, the energy savings achieved by *simple*, *dedicated-classic*, and *shared-classic* models are shown. Column $\%E_c$ represents the ratio between the energy consumption of the optimized vs the full active network. Column gap_{opt} represents the gap of the final solution w.r.t. to the best lower bound computed by CPLEX. Column gap_{simple} represents the relative increase of energy consumption due to the survivability requirement: it is computed as $E_c^{prot} - E_c^{simple}/E_c^{simple}$, where $\%E_c^{prot}$ and $\%E_c^{prot^{simple}}$ represent the energy consumption of the optimized network w.r.t. the full active one, for the unprotected and protected case, respectively. As expected, the explicit implementation of a protection scheme increases the network energy consumption, in fact the energy-aware approaches keep activated additional resources to cope with possible failures. In the case without protection, the consumption E_c varies from 50.1% to 60.6%, in the *dedicated-classic* case network consumption is between 61.4% and 71.4%, with absolute and relative increase, on average, of 10% and 20%, respectively. By considering the more sophisticated *shared-classic* protection, the consumption can be reduced, w.r.t. the *dedicated-classic* case, up to 5%. However, while for the *dedicated-classic*, the model computes nearly optimal solutions within the time limit of one hour (gap_{opt} usually lower than 1% and never above 3.5%), for the *shared-classic* case the gap from the best lower bound is in some instances larger than 15% (Instances 6–7), as the model is more complex and requires a high computational effort. For this reason, in some instances the reported difference between shared and dedicated protection consumption is smaller than 1% (Instances 6–7–11).

To overcome this problem, the single time period heuristic can be applied. Heuristic results are reported in Tables 9 and 10.In Table 9 we analyze the gap between exact model and STPH solutions. Columns $Heur_{gap}$ represent the difference between the energy consumption obtained by the model and that achieved by STPH, i.e. $E_c^{heur} - E_c^{model}$. In Table 10 we compare the saving improvement achieved by the smart protection solution produced by STPH w.r.t. the classic one. Columns $\Delta_{smart}^{classic}$ represent the absolute difference between the energy consumption obtained with the smart and the classic models. The time limits are reported, as well: in Tables 9 and 10, differently from Tables 7 and 8, *TL* represent the time limit imposed to CPLEX when solving a single time period of STPH.

Table 9 shows that, by using STPH with a time limit of 6 min, we reduce the energy consumption of the solutions with shared protection up to about 5% (Instances 3–6–7–11). The difference between shared and dedicated protection for the instances for which the gap obtained solving the model is large (Instances 6–7–11) is therefore increased. Furthermore, it is worth pointing out that, even for the instances of the dedicated case solved at optimality or with a very small gap using the complete model, the gap between STPH and the formulation is very small, varying between 0.6% and −0.2%, negative values meaning that STPH solutions improve upon the sub-optimal solutions found by CPLEX when solving the model. Having shown the good quality of STPH algorithm solutions in the remainder of this section we report only the results obtained by solving STPH, for practical and space reasons. The possibility of putting to sleep the line cards carrying only the backup links (*smart* protection) is expected to substantially decrease the energy consumption of the network w.r.t. the *classic* case. This hypothesis is clearly confirmed by the results of Table 10, where we observe that *smart* protection allows to reduce the consumption of the protected solutions (w.r.t. the total network consumption) by up to 7.1% and 3.9%, for the dedicated and shared case,

Table 10
Comparison between the energy saving achieved by STPH with classic and smart protection schemes, `polska` instances.

ID	Polska – STPH – classic vs smart			
	Dedicated		Shared	
	$\Delta_{smart}^{classic}$ (%)	*TL* (s)	$\Delta_{smart}^{classic}$ (%)	*TL* (s)
1	−3.9	30	−1.9	360
2	−3.5	30	−2.2	360
3	−3.2	30	−1.9	360
5	−7.1	30	−3.4	360
6	−5.9	30	−3.9	360
7	−5.5	30	−3.6	360
9	−4.2	30	−2.0	360
10	−3.8	30	−2.3	360
11	−3.5	30	−2.1	360

Table 8
Comparison between simple and protected solutions obtained by solving the exact model with 1 h time limit with `polska` instances.

ID	*TL* (h)	Polska – exact model							
		Simple case		Dedicated prot classic			Shared prot classic		
		$\%E_c$	gap_{opt} (%)	$\%E_c$	gap_{opt} (%)	gap_{simple} (%)	$\%E_c$	gap_{opt} (%)	gap_{simple} (%)
1	1	60.6	1.3	71.4	1.4	17.8	66.9	3.6	10.3
2	1	60.5	0.9	71.3	0.9	17.8	66.3	4.4	9.6
3	1	60.3	0.6	71.4	0.7	18.4	70.4	8.9	16.7
5	1	50.7	2.4	62.2	2.6	22.7	59.3	10.1	17.0
6	1	50.1	0.8	61.4	3.3	22.7	60.3	15.5	20.5
7	1	50.3	0.4	61.7	2.7	22.6	61.7	15.8	22.6
9	1	60.0	1.4	70.9	0.9	18.1	66.2	3.2	10.3
10	1	59.8	0.7	70.7	0.8	18.1	65.7	3.6	9.8
11	1	59.7	0.0	70.8	0.5	18.6	70.9	11.1	18.8

Table 9
Comparison between the energy saving achieved by solving the exact model and running the single time period heuristic with different types of protection, `polska` instances.

ID	TL_{model} (h)	Polska – exact model vs STPH					
		Simple case		Dedicated prot classic		Shared prot classic	
		$Heur_{gap}$ (%)	*TL* (s)	$Heur_{gap}$ (%)	*TL* (s)	$Heur_{gap}$ (%)	*TL* (s)
1	1	0.00	60	0.1	30	−0.3	360
2	1	0.25	60	0.1	30	−0.3	360
3	1	0.16	60	0.0	30	−4.0	360
5	1	0.41	60	0.6	30	−2.1	360
6	1	0.00	60	−0.1	30	−3.6	360
7	1	0.28	60	−0.2	30	−4.5	360
9	1	0.28	60	0.1	30	−0.3	360
10	1	0.28	60	0.2	30	−0.4	360
11	1	0.17	60	0.1	30	−4.9	360

respectively. *Smart shared* produces smaller energy consumption reduction, w.r.t. the non smart case, than *smart dedicated*. The smaller improvement obtained by the smart scheme with shared protection w.r.t. dedicated protection is explained by the smaller amount of backup capacity that can be put to sleep. The most important result that is worth pointing out here is that with the smart scheme, dedicated protection can be more energy efficient than classic shared protection, while being less computationally expensive and easier to implement.

8.2.3. Protection strategies: congestion analysis

Concerning the congestion, it is necessary to remind that shared protection, due to the high efficiency of the backup allocation scheme, can deal with levels of traffic that cannot be managed by the dedicated protection scheme, without violating the maximum utilization constraints. To compute $\varpi^{85\%}_{50\%}$, shared instead of dedicated protection can be used. If shared protection is chosen, $\varpi^{85\%}_{50\%}$ increases up to 25%. Therefore, although the computational effort required to handle shared protection is significantly higher than in the dedicated case, shared protection is worth being implemented to further reduce network congestion.

To better understand the balance between network congestion and energy savings, we report in Fig. 4 the network energy-consumption computed by varying the secondary maximum utilization threshold μ_b from 0.5 to 1. In this specific set of tests, we considered *dedicated* protection and traffic matrices obtained by using $\varpi^{50\%}_{50\%}$ instead of the $\varpi^{85\%}_{50\%}$. In fact, with $\varpi^{85\%}_{50\%}$ the problem would not be feasible in case of $\mu_b < 0.85$. Fig. 4 shows that the difference between the network consumption obtained with $\mu_b = 0.5$ and $\mu_b = 1$ varies from 4% to 8%. The plot clearly shows how a network provider can balance energy savings and network congestion according to his own requirements.

8.2.4. Joint protection and robustness

To conclude the analysis on the `polska` instances, let us analyze the results on the *robust dedicated* case solved with the exact formulation, reported in Table 11. As for the simple *robust* case, it is possible to obtain solutions completely immunized to traffic variation ($\%_{infeas} = 0\%$) where the power consumption is increased, on average of 1% and in the worst case of 2.6% (Instance 8, $\bar{r}^{\sigma}_{d} = 0.2$). Furthermore, the energy consumption reduction obtained by the smart approach w.r.t. the classic one, is about 4% and up to 6% (similar to the protected non robust case).

Finally, Fig. 5 reports the average energy savings obtained with the three scenarios *a*, *b*, and *c*. It is possible to observe that the final energy consumption for `polska` computed by varying the protection degree follows the expected trend previously showed in Fig. 3.

For comparison purposes, we include in the figure the network power consumption observed for a *benchmark* case: *simple* problem with fixed routing configuration for the entire time-horizon. The *benchmark* routing configuration is computed by solving the following MILP formulation:

$$\min \ \mu \tag{33}$$

s.t.

$$\sum_{(i,j)\in A} x^d_{ij} - \sum_{(j,i)\in A} x^d_{ji} = b^d_i, \qquad \forall i \in N, \quad d \in D \tag{34}$$

$$\mu \geqslant \frac{\sum_{d\in D} \rho_d x^d_{ij}}{n_{ij}\gamma}, \quad \forall (i,j) \in A \tag{35}$$

$$\mu \leqslant 0, \quad \forall (i,j) \in A \tag{36}$$

whose goal is to optimize the network routing so as to minimize the maximum link utilization of the fully active network within a single period. The bandwidth requirement of each traffic demand $d \in D$ is equal to the nominal value ρ_d. The above formulation represents a traditional traffic engineering problem with no energy-related aspects. The obtained routing paths are then maintained for the whole time-horizon. The redundant chassis which are not used by such paths are put in sleep state along the entire day, while on each link the number of active line cards is chosen according to the amount of traffic carried by each link within each time period. All the inter-period constraints are respected.

The power savings achieved by the *benchmark* solutions, which do not consider protection or robustness, are significantly lower than those observed when the energy-aware framework is applied even with all the survivability features, i.e. *robust plus dedicated classic* problem. Thus, although minor savings can be naturally achieved by exploiting network redundancies and bundled links, a significant improvement is observed when both energy-aware and performance aspects are jointly optimized. We refer the reader to [11] for exhaustive comparisons

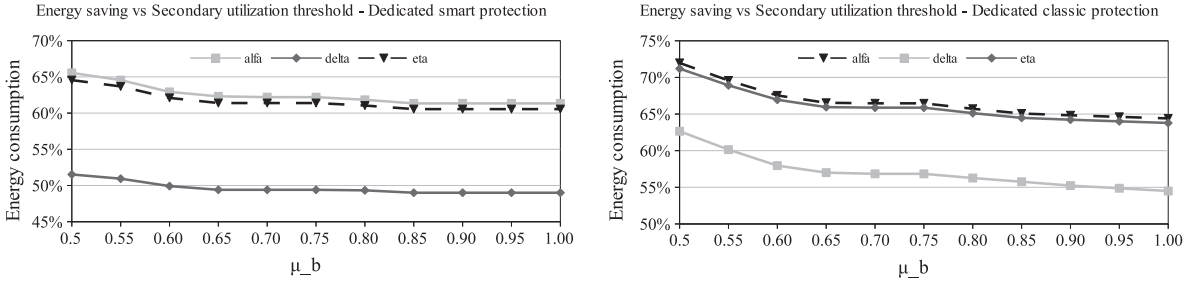

Fig. 4. Analysis of the trade-off between energy savings and network congestion, obtained by adjusting the secondary utilization threshold μ_b from 0.5 to 1 when solving STPH.

Table 11
Robustness analysis for the solutions obtained by the robust exact model with classic dedicated protection with 1 h time limit on `polska` instances.

ID	$\hat{r}$	*TL* (h)	Polska – exact model – robust approach with dedicated protection											
			$\Gamma = 0$			$\Gamma = 1$			$\Gamma = 3$			$\Gamma = 5$		
			$\%E_c$	$\%_{infeas}$	$\Delta_{smart}^{classic}$ (%)	$\%E_c$	$\%_{infeas}$	$\Delta_{smart}^{classic}$ (%)	$\%E_c$	$\%_{infeas}$	$\Delta_{smart}^{classic}$ (%)	$\%E_c$	$\%_{infeas}$	$\Delta_{smart}^{classic}$ (%)
4	0.05	1	70.6	96.7	−3.1	71.4	17.9	−3.4	71.5	0.5	−3.4	71.6	0.0	−3.5
4	0.10	1	70.6	98.7	−3.1	71.4	61.7	−3.2	71.6	1.2	−3.3	71.8	0.0	−3.4
4	0.15	1	70.6	99.8	−3.1	71.6	63.2	−3.4	71.9	0.7	−3.3	72.1	0.0	−3.3
4	0.20	1	70.6	99.7	−3.1	71.6	64.1	−3.2	72.1	3.5	−3.1	72.6	0.0	−3.4
8	0.05	1	60.8	95.7	−5.5	61.8	31.9	−6.2	61.8	0.4	−5.7	62.0	0.0	−6.0
8	0.10	1	60.8	99.1	−5.5	61.8	38.6	−5.7	62.3	1.9	−5.4	62.3	0.0	−5.9
8	0.15	1	60.8	99.0	−5.5	61.8	63.8	−5.8	62.6	1.8	−5.8	63.2	0.0	−6.2
8	0.20	1	60.8	99.8	−5.5	62.0	55.4	−5.5	62.9	2.8	−5.3	63.4	0.0	−5.5
12	0.05	1	70.0	91.4	−3.2	70.9	21.4	−3.7	70.9	0.9	−3.4	71.0	0.0	−3.7
12	0.10	1	70.0	97.4	−3.2	70.9	32.3	−3.5	71.0	1.0	−3.4	71.3	0.0	−3.7
12	0.15	1	70.0	99.0	−3.2	71.0	56.2	−3.5	71.4	1.5	−3.4	71.5	0.0	−3.5
12	0.20	1	70.0	99.4	−3.2	71.0	71.3	−3.4	71.6	2.1	−3.3	71.9	0.0	−3.5

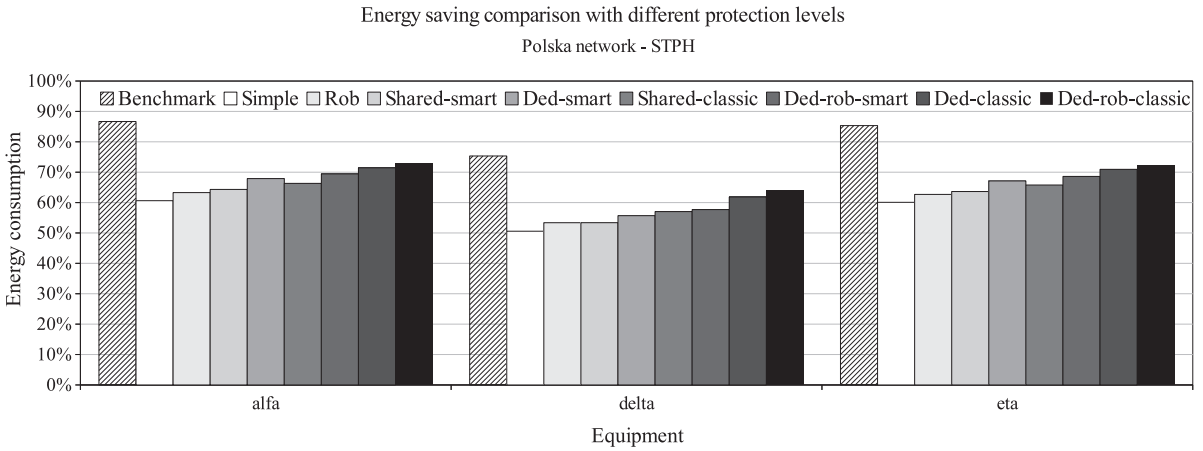

Fig. 5. Energy savings achieved by STPH when implementing the different protection schemes on `polska` instances.

between optimized solutions obtained by considering different routing limitations.

8.3. Largest networks

In the second group of tests, we experimented with `nobel-germany`, `nobel-eu` and `germany` network by running STPH or STPH-RP (the restricted path version of STPH). For comparison purposes, a restricted set of instances were tested with both procedures. STPH-RP was then used to solve instances that were too computationally demanding to be efficiently solved in a reasonable amount of time by the simple STPH. The time limit for the single time period used to run STPH and STPH-RT are reported in Table 12. If a method cannot provide a feasible solution for an instance a "/" is reported in the corresponding entry of the table (only STPH can provide feasible solutions for instance `nobel-germany`).

Fig. 6 reports the results for the `nobel-germany` network, while Fig. 7 reports the results for the `nobel-eu` network.

First of all, we can observe that the consumption trend showed in Fig. 5, is confirmed in Figs. 6 and 7, where we report the network consumption obtained by STPH on `nobel-germany` and `nobel-eu` networks considering different protection cases. The only difference that can be observed is that the energy consumption for the *dedicated-smart* case is on average smaller than the one of the *shared-classic* case. This can be explained as the solver is not able to efficiently solve the shared protection model, even for the single period, and to obtain a small gap when the instance dimensions increase. It is worth noting that, in some tests, the solution computed by the warm start procedure cannot be improved by the solver within the chosen time-limit. Besides, due to memory limits (8 GB of RAM), the shared protection instances could not even be initialized for the `nobel-eu` and `germany` networks. Thus, as a solution feasible for the dedicated problem is naturally feasible for the shared one, the solutions obtained by solving the *dedicated* problem are applied also for the shared case. By solving STPH, the consumption difference between the simple case and the most protected one, i.e. the *dedicated-classic robust*, is around 20% for both `nobel-germany`, `nobel-eu` networks.

In Figs. 8 and 9, the network energy consumption, the infeasibility degree and the maximum threshold overrun are represented for the robust case (in Table 7, the last two values are indicated as $\%_{infeas}$ and Max_{dev}). The four graphics

clearly prove that our approach allow to efficiently manage traffic variations without considerably increasing the network consumption (increase lower than 2% for solution completely immunized). It is also worth pointing out that by simply increasing Γ from 0 (no robustness) to 1, we are already able to substantially immunize the solution, with $\%_{infeas}$ improved from 90% to around 15%. The results for the *eta* case are very similar and therefore not reported.

For the *dedicated robust case*, the medium size `nobel-eu` network was solved using the restricted-path version of STPH, for efficiency reasons. With the aim of evaluating the efficiency of STPH-RP in Fig. 10 the consumption obtained with both STPH and STPH-RP (with $\Omega = 10$) considering `nobel-eu` network and *dedicated classic* protection are reported. The consumption difference between the two solution methods is generally slightly lower than 10%. Therefore, taking into account all the paths allows to gain a substantial amount of savings when handling small and medium size instances. However, the use of a restricted set of paths turned out to be a reasonable strategy to reduce the computational effort when dealing with larger instances without excessively degrading the achieved energy savings.

Finally, to further confirm the good performance of STPH-RP, the average network consumption values

Table 12
CPLEX time limits for the single time period to solve `nobel-germany`, `nobel-eu` and `germany` instances with different types of protection.

	Simple		Robust		Dedicated		Shared		Robust-dedicated	
Net	TL_{STPH} (s)	$TL_{STPH-RP}$ (s)	TL_{STPH} (s)	$TL_{STPH-RP}$ (s)	TL_{STPH} (s)	$TL_{STPH-RP}$ (s)	TL_{STPH} (s)	$TL_{STPH-RP}$ (s)	TL_{STPH} (s)	$TL_{STPH-RP}$ (s)
Nobel-ger	60	/	90	/	90	/	360	/	120	/
Nobel-eu	300	/	300	/	300	300	/	/	1200	/
Germany	/	600	/	600	/	600	/	/	/	1200

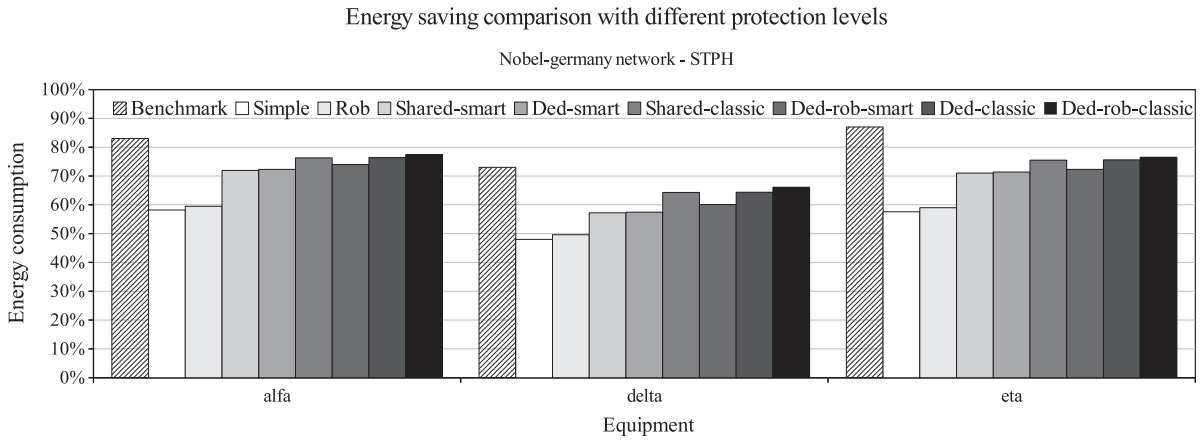

Fig. 6. Energy savings achieved by STPH when implementing the different protection schemes on `nobel-germany` instances.

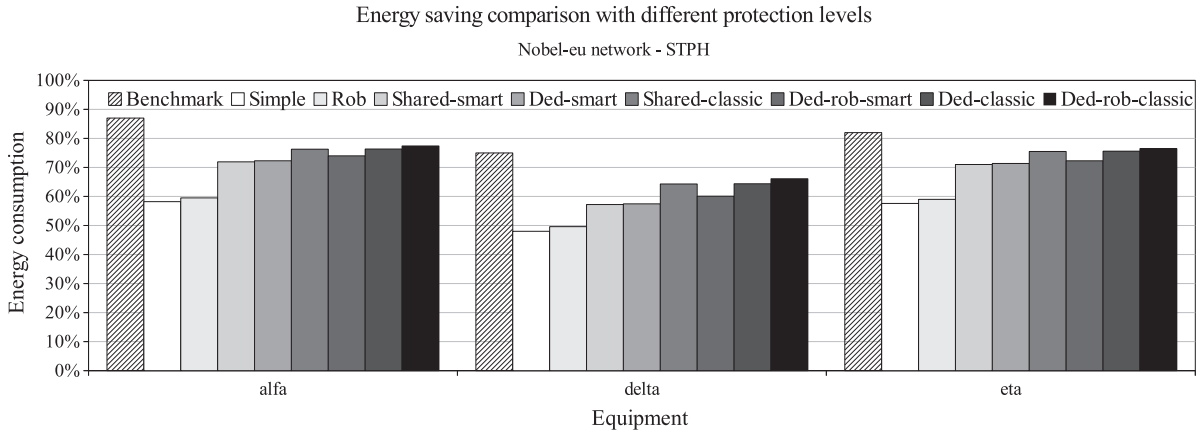

Fig. 7. Energy savings achieved by STPH when implementing the different protection schemes on `nobel-eu` instances. The $*$ in the graph legend is used for the instances solved, due to complexity issues, with STPH-RP using $\Omega = 10$.

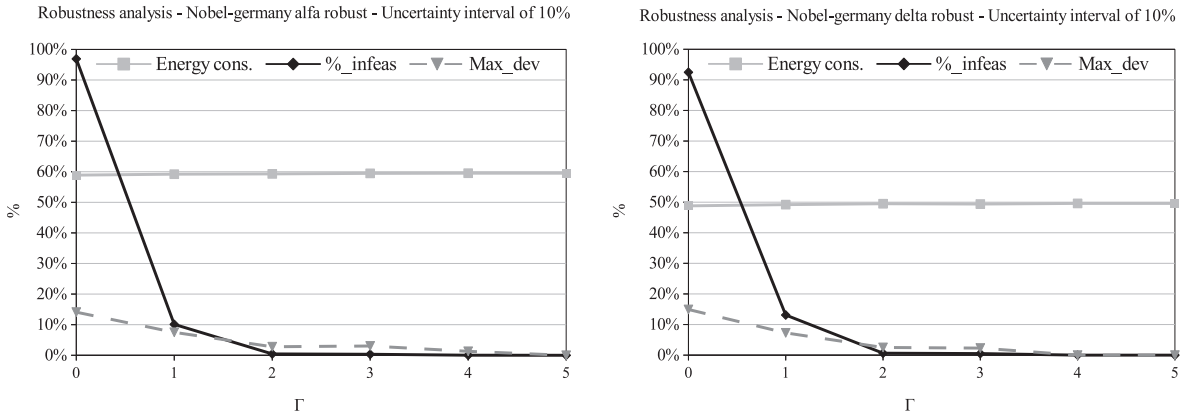

Fig. 8. Energy savings achieved by STPH when implementing the robust scheme on `nobel-germany` instances.

computed on the `germany` network with all the different protection schemes are reported in Fig. 11. We solved the instances with STPH-RP with $\Omega = 5$. Also in this case the heuristic method provides significant savings, obtaining final network consumption from 60% up to 80% of the original value.

8.4. Economic evaluation

Computational results obtained by experimenting with realistic daily traffic profiles show how the energy consumption of current backbone IP networks can be reduced from 30% up to 50%. The amount of savings is strictly related to the level of survivability and to the ratio between the consumption of line cards and chassis. Let us quantify the economic savings achieved. Let `germany` with *delta* configuration be our reference network (this is the largest network of our test-bed in its most consuming configuration). When fully active, the network consumes

$$\text{Daily consumption} = 2\left(\sum_{i\in N}\bar{\pi}_i + \sum_{(i,j)\in A}\pi_{ij}n_{ij}\right)\sum_{\sigma\in S}h_\sigma \qquad (37)$$

Being $\bar{\pi}_i = 86.4\,W$, $\pi_{ij} = 18.6\,W$, $n_{ij} = 2$ and $\sum_{\sigma\in S}h_\sigma = 24\,h$, the total daily consumption is equal to 521 KW h (the whole consumption is multiplied by two to take into account cooling equipment). Thus, being the electricity cost equal to 0.20 € per KW h (see [51]), the yearly consumption of 521 KW h × 365 = 190.165 MW h results in a yearly electricity bill of 38,033 €. In that case, the energy-aware network management framework would allow to save between about 10,000 € (*robust plus dedicated-classic*) and about 20,000 € (*simple*).

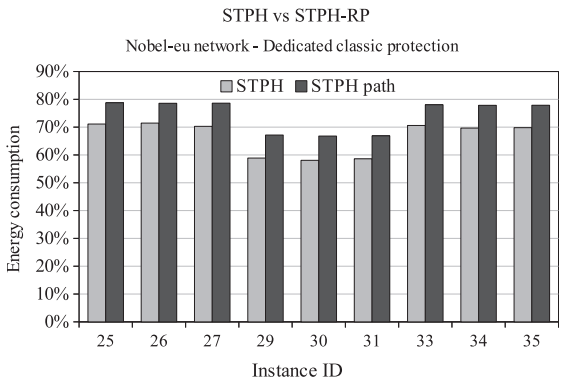

Fig. 10. Energy saving comparison between STPH and STPH-RP on `nobel-eu` network with *dedicated classic* protection.

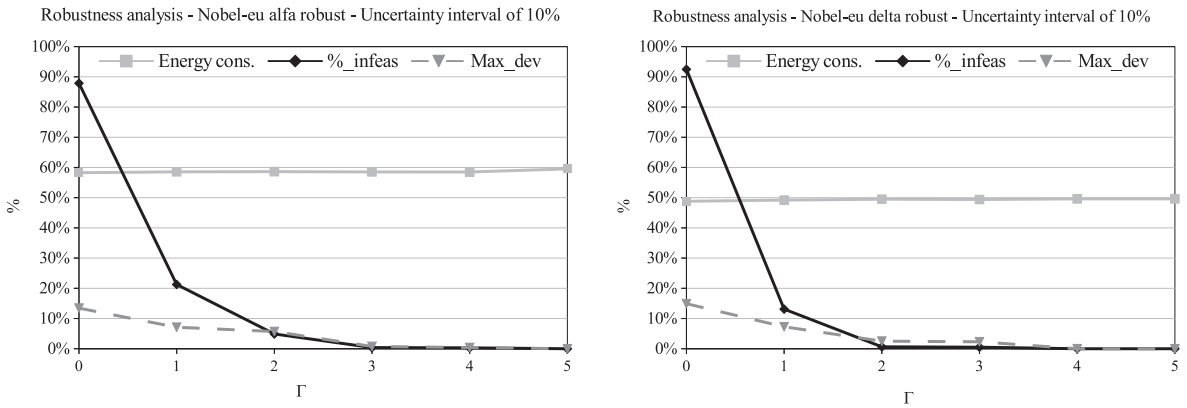

Fig. 9. Energy savings achieved by STPH when implementing the robust scheme on `nobel-eu` instances.

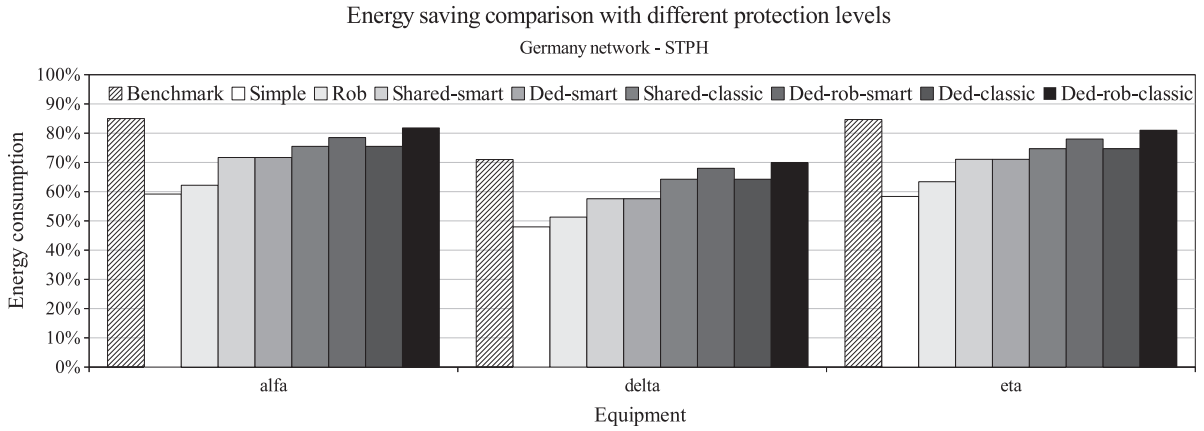

Fig. 11. Energy savings achieved by STPH-RP with $\Omega = 5$ when implementing the different protection schemes on `germany` instances.

In our experimental scenarios we considered network devices characterized by a limited capacity, and consequently by a limited power consumption. The traffic was then scaled to model realistic workload conditions (with maximum utilization close to 50% during peak periods). Assume now to equip each network node with a Juniper T640 chassis (hourly consumption of 1114 W) and each link $(i,j) \in A$ with n_{ij} Type-4 FPC, 40 Gbps full duplex line cards (hourly consumption of 394 W) [52]: in this case the yearly power consumption amounts to 3.4 GW h, with an electricity bill of 681,000 €. Therefore, monetary savings would amount to at least 300,000 € per year for a single backbone network.

9. Concluding remarks

In this paper, the issues of energy savings and network resilience to both failures and traffic variations have been thoroughly investigated. We have proposed a comprehensive set of modeling tools to efficiently perform off-line multi-period energy-aware network management without compromising the normal network operation. We have presented and discussed both exact and heuristic methods able to put to sleep network line cards and chassis while reserving backup resources to efficiently cope with single link failures and leaving enough spare capacity to absorb the unexpected peak of traffic. Extensive experimentations have shown that even when full protection is guaranteed (dedicated protection with robustness to traffic variations) it is possible to save up to 30% of the daily network consumption.

References

[1] GreenTouch consortium. <www.greentouch.org>.

[2] S. Lambert, W. Van Heddeghem, W. Vereecken, B. Lannoo, D. Colle, M. Pickavet, J. Ferry, Worldwide electricity consumption of communication networks, Opt. Exp. 20 (26) (2012) B513–B524.

[3] H. Mellah, B. Sansò, Review of facts, data and proposals for a greener Internet, in: IEEE Broadnets, Sixth International Conference on Broadband Communication Networks and Systems, September 2009, pp. 1–5.

[4] R. Bolla, R. Bruschi, F. Davoli, F. Cucchietti, Energy efficiency in the future internet: a survey of existing approaches and trends in energy-aware fixed network infrastructures, IEEE Commun. Surv. Tutorials 13 (2) (2011) 223–244.

[5] P. Vetter, L. Lefevre, L. Gasca, K. Kanonakis, L. Kazovsky, B. Lannoo, A. Lee, C. Monney, X. Qiu, F. Saliou, et al., Research roadmap for green wireline access, in: IEEE International Conference on Communications (ICC), 2012, IEEE, 2012, pp. 5941–5945.

[6] E. Amaldi, A. Capone, L.G. Gianoli, Energy-aware IP traffic engineering with shortest path routing, Comput. Netw. 57 (6)(2013) 1503–1517.

[7] J. Chabarek, J. Sommers, P. Barford, C. Estan, D. Tsiang, S. Wright, Power awareness in network design and routing, in: Proceedings of INFOCOM 08, Phoenix, Arizona, 2008, pp. 457–465.

[8] P. Mahadevan, P. Sharma, S. Banerjee, P. Ranganathan, A power benchmarking framework for network devices, in: Proc. of the 8th International IFIP-TC 6 Networking Conference, May 2009, pp. 795–808.

[9] A.P. Bianzino, C. Chaudet, D. Rossi, J-L. Rougier, A survey of green networking research, IEEE Commun. Surv. Tutorials 14 (1) (2012) 3–20.

[10] S. Zeadally, S.U. Khan, N. Chilamkurti, Energy-efficient networking: past, present, and future, J. Supercomput. (2011) 1–26.

[11] B. Addis, A. Capone, G. Carello, L.G. Gianoli, B. Sanso, Energy management through optimized routing and device powering for greener communication networks, IEEE/ACM Trans. Netw. 22 (1) (2014) 313–325.

[12] M.R. Garey, D.S. Johnson, Computers and Intractability. A Guide to Theory of NP-Completeness, W.H. Freeman and Co., 1979.

[13] N. Vasić, D. Kostić, Energy-aware traffic engineering, in: Proc. of the 1st International Conference on Energy-Efficient Computing and Networking, ACM, 2010, pp. 169–178.

[14] Aruna Prem Bianzino, Luca Chiaraviglio, Marco Mellia, Jean-Louis Rougier, Grida: green distributed algorithm for energy-efficient IP backbone networks, Comput. Netw. 56 (14) (2012) 3219–3232.

[15] B. Addis, A. Capone, G. Carello, L.G. Gianoli, B. Sansò, Multi-period traffic engineering of resilient networks for energy efficiency, in: Proc. of GreenCom-12, IEEE Online Conference on Green Communications, 26–28 September, 2012.

[16] B. Addis, A. Capone, G. Carello, L.G. Gianoli, B. Sansò, Energy aware management of resilient networks with shared protection, in: Proc. of SustainIT-12, the Second IFIP/IEEE Conference on Sustainable Internet and ICT for Sustainability, October 2012, pp. 1–9.

[17] B. Addis, A. Capone, G. Carello, L.G. Gianoli, B. Sansò, A robust optimization approach for energy-aware routing in MPLS networks, in: Proc. of ICNC-13, International Conference on Computing, Networking and Communications, Green Computing, Networking and Communications Symposium, 28–31 January, IEEE, San Diego, USA, 2013.

[18] D. Bertsimas, D.B. Brown, C. Caramanis, Theory and applications of robust optimization, SIAM Rev. 53 (3) (2011) 464–501.

[19] M. Gupta, S. Singh, Greening of the internet, in: Proceedings of the conference on applications, technologies, architectures, and protocols for computer communications, 2003, pp. 19–26.

[20] L. Chiaraviglio, D. Ciullo, M. Mellia, M. Meo, Modeling sleep mode gains in energy-aware networks, Comput. Netw. 57 (15) (2013) 3051–3066.

[21] L. Chiaraviglio, A. Cianfrani, E.L. Rouzic, M. Polverini, Sleep modes effectiveness in backbone networks with limited configurations, Comput. Netw. 57 (15) (2013) 2931–2948.

[22] B. Addis, A. Capone, G. Carello, L.G. Gianoli, B. Sansò, Energy-aware multiperiod traffic engineering with flow-based routing, in: ICC 2012, Workshop on Green Communications and Networking, June 2012, pp. 5957–5961.
[23] F. Francois, N. Wang, K. Moessner, S. Georgoulas, Optimizing link sleeping reconfigurations in ISP networks with off-peak time failure protection, IEEE Trans. Netw. Serv. Manage. 10 (2) (2013) 176–188.
[24] L. Chiaraviglio, M. Mellia, F. Neri, Minimizing ISP network energy cost: formulation and solutions, IEEE/ACM Trans. Netw. (TON) 20 (2) (2012) 463–476.
[25] R.G. Garroppo, S. Giordano, G. Nencioni, M. Pagano, M.G. Scutellá, Network power management: models and heuristic approaches, in: 2011 IEEE Global Telecommunications Conference – GLOBECOM 2011, IEEE, 2011, pp. 1–5.
[26] A. Coiro, M. Listanti, A. Valenti, F. Matera, Energy-aware traffic engineering: a routing-based distributed solution for connection-oriented IP networks, Comput. Netw. 57 (9) (2013) 2004–2020.
[27] W. Fisher, M. Suchara, J. Rexford, Greening backbone networks, in: Proceedings of the First ACM SIGCOMM Workshop on Green Networking – Green Networking '10, ACM Press, 2010, p. 29.
[28] G. Lin, S. Soh, K. Chin, M. Lazarescu, Efficient heuristics for energy-aware routing in networks with bundled links, Comput. Netw. 57 (8) (2013) 1774–1788.
[29] J. Galán-Jiménez, A. Gazo-Cervero, Using bio-inspired algorithms for energy levels assessment in energy efficient wired communication networks, J. Netw. Comput. Appl. 37 (2014) 171–185.
[30] S.S.W. Lee, P.K. Tseng, A. Chen, Link weight assignment and loop-free routing table update for link state routing protocols in energy-aware internet, Future Gener. Comput. Syst. 28 (2) (2012) 437–445.
[31] A. Capone, D. Corti, L.G. Gianoli, B. Sansò, An optimization framework for the energy management of carrier ethernet networks with multiple spanning trees, Comput. Netw. 56 (17) (2012) 3666–3681.
[32] A. Capone, C. Cascone, L.G. Gianoli, B. Sanso, OSPF optimization via dynamic network management for green IP networks, in: 2013 Sustainable Internet and ICT for Sustainability (SustainIT), IEEE, 2013, pp. 1–9.
[33] M. Shen, H. Liu, K. Xu, N. Wang, Routing on demand: toward the energy-aware traffic engineering with OSPF, in: NETWORKING 2012, 2012, pp. 232–246.
[34] B. Sansò, H. Mellah, On reliability, performance and Internet power consumption, in: DRCN09, Seventh International Worshop of the Design of Reliable Communication Networks, October 2009, pp. 259–264.
[35] A. Muhammad, P. Monti, I. Cerutti, L. Wosinska, P. Castoldi, A. Tzanakaki, Energy-efficient WDM network planning with dedicated protection resources in sleep mode, in: Proc. of GLOBECOM 2010, Global Telecommunications Conference, IEEE, 2010, pp. 1–5.
[36] A. Jirattigalachote, C. Cavdar, P. Monti, L. Wosinska, A. Tzanakaki, Dynamic provisioning strategies for energy efficient WDM networks with dedicated path protection, Opt. Switch. Netw. 8 (3) (2011) 201–213.
[37] N. Bao, L. Li, H. Yu, Z. Zhang, H. Luo, Power-aware provisioning strategy with shared path protection in optical WDM networks, Opt. Fiber Technol. 18 (2) (2012) 81–87.
[38] R. He, B. Lin, Dynamic power-aware shared path protection algorithms in WDM mesh networks, J. Commun. 8 (1) (2013) 55–65.
[39] G. Wu, G. Mohan, Power efficient integrated routing with reliability constraints in ip over WDM networks, in: IEEE International Conference on Communication Systems (ICCS), IEEE, 2012, pp. 275–279.
[40] A. Aldraho, A.A. Kist, Enabling energy efficient and resilient networks using dynamic topologies, in: Sustainable Internet and ICT for Sustainability (SustainIT), IEEE, 2012, pp. 1–8.
[41] B. Luo, W. Liu, A. Al-Anbuky, Energy aware survivable routing approaches for next generation networks, in: 2013 Australasian Telecommunication Networks and Applications Conference (ATNAC), Ieee, 2013, pp. 160–165.
[42] S.S.W. Lee, K. Li, A. Chen, Survivable green active topology design and link weight assignment for ip networks with NotVia fast failure reroute, in: 2013 IEEE International Conference on Communications (ICC), IEEE, 2013, pp. 3575–3580.
[43] M. Pióro, D. Medhi, Routing, Flow and Capacity Design in Communication and Computer Networks, Morgan Kaufman, 2004.
[44] D. Coudert, A.M. Koster, T.K. Phan, M. Tieves, Robust redundancy elimination for energy-aware routing, in: 2013 IEEE International Conference on Green Computing and Communications and IEEE Internet of Things and IEEE Cyber, Physical and Social Computing, number GreenCom, IEEE, 2013, pp. 179–186.
[45] A. Ben-Tal, L. El Ghaoui, A. Nemirovski, Robust Optimization, Princeton University Press, 2009.
[46] A. Mackarel, et al., Study of Environmental Impact, DN3.5.2, GEANT Project, May 2011.
[47] Introduction to Cisco IOS NetFlow – A Technical Overview. Tech. Rep., Cisco Systems, 2012.
[48] P. Casas, S. Vaton, L. Fillatre, L. Chonavel, Efficient methods for traffic matrix modeling and on-line estimation in large-scale IP networks, in: Proc. of 21st International Teletraffic Congress, ITC 2009, IEEE, 2009, pp. 1–8.
[49] Active/Idle Toggling with 0BASE-x for Energy Efficient Ethernet, Presentation to the IEEE 802.3az Task Force, November 2007.
[50] S. Orlowski, R. Wessäly, M. Pióro, A. Tomaszewski, SNDlib 1.0 survivable network design library, Networks 55 (3) (2010) 276–286.
[51] J.C. Cardona Restrepo, C.G. Gruber, C. Mas Machuca, Energy profile aware routing, in: 2009 IEEE International Conference on Communications Workshops, IEE, 2009, pp. 1–5.
[52] W. Van Heddeghem, F. Idzikowski, W. Vereecken, D. Colle, M. Pickavet, P. Demeester, Power consumption modeling in optical multilayer networks, Photon Netw. Commun. 24 (2) (2012) 86–102.